

# The Fourier modal method for gratings with bi-anisotropic materials

Ilia Smagin,<sup>\*</sup> Sergey Dyakov,<sup>†</sup> and Nikolay Gippius  
*Skolkovo Institute of Science and Technology*

We report an advanced formulation of the Fourier modal method developed for two-dimensionally periodic multilayered structures containing materials with non-zero macroscopic magneto-electric coefficients (also known as coefficients of chirality and bi-anisotropy) represented as arbitrary  $3 \times 3$  tensors. We consider two numerical schemes for this formulation: with and without Lifeng Li's factorization rules. For both schemes, we provide explicit expressions for the Fourier tensors of macroscopic material parameters and demonstrate that, in the absence of magneto-electric coupling, they reduce to conventional Li's operators. We show that the scheme employing factorization rules facilitates improved convergence, even when the macroscopic chirality coefficient is large. The described formulation represents the fast and rigorous technique for theoretical studies of periodic structures with chiral, bi-anisotropic, or non-reciprocal materials in the widely used framework of the Fourier modal method.

## I. INTRODUCTION

The electrodynamic semi-analytical Fourier modal method (FMM) is one of the most efficient and fastest approaches for theoretical studies of the optical properties of layered periodic structures in photonics. This technique employs a scattering matrix formalism along with the Fourier decomposition of fields in each of the vertically homogeneous layers. Since publication of the seminal works [1, 2], this technique has undergone extensive enhancements and adaptations [3, 4].

To our knowledge, most implementations of the FMM are based on constitutive relations that connect the local electric induction with the local electric field and the local magnetic induction with the local magnetic field. Typically, this form of constitutive relation serves as an excellent approximation for local polarization and magnetization, accurately describing experimental observations. However, there is a class of optical phenomena that cannot be described by these relations. Among these phenomena are circular dichroism — the difference in the absorption of left and right circularly polarized light by a substance [5–7], and optical activity — the rotation of the polarization plane of linearly polarized light as it travels through the substance [8, 9]. Microscopically, these phenomena originate from the broken inversion symmetry (chirality) of molecules that constitute such substances. Circular dichroism and optical activity can be described by the simplest form of constitutive relations only by using the dielectric permittivity dependent on the polarization state of light. Although this phenomenological approach can be effective in homogeneous media, it fails in periodic media with intrinsically chiral materials.

Comprehensive research on the optical properties of chiral materials in the past century [10, 11] can be summarized in constitutive relations containing cross-coupling coefficients between local electric induction and

the local magnetic field and local magnetic induction and the local electric field. These cross-coupling coefficients are referred to as macroscopic chirality coefficients, which, along with dielectric permittivity and magnetic permeability, are subject to experimental determination. In natural chiral materials, macroscopic chirality coefficients have relatively small absolute values, typically ranging between  $10^{-4}$  and  $10^{-5}$ . In principle, this allows one to utilize perturbation theory for the generalization of the FMM, since the cross-terms in the constitutive equations are significantly smaller compared to the main terms [12]. However, this method will be inadequate for describing resonant scenarios when the chirality coefficients have poles in their frequency dependences. In addition, artificial chiral materials, such as metamaterials, may also have large chirality coefficients that can make the use of perturbation theory insufficient. Thus, the development of the Fourier modal method capable of calculating the scattering matrix of the multilayered structure with chiral substances is of great importance. This is further stimulated by the growing interest of the photonics community in chiral polaritonics, which is in its infancy at the moment.

As shown in [11], constitutive relations with magneto-electric coupling coefficients can describe not only chiral media but also media for which the electromagnetic reciprocity theorem does not hold. Non-reciprocal media require not only broken inversion symmetry, but also broken time-reversal symmetry, which can be achieved by static magnetic field, rotation, or some other external influence [13].

Chiral and nonreciprocal media are special cases of a more general class of magneto-electric media; the wide variety of optical phenomena associated with these media can be described by constitutive relations with magneto-electric coupling. Although an improvement of the FMM applicable to structures containing magneto-electric but homogeneous layers is quite straightforward [14], the generalization of the FMM to magneto-electric periodic media is much more challenging due to the necessity of using Li's factorization rules for convergence improvement [15–17]. In this paper, we address this problem and formulate

<sup>\*</sup> Ilia.Smagin@skoltech.ru

<sup>†</sup> S.Dyakov@skoltech.ru

the FMM considering macroscopic dielectric permittivity, magnetic permeability, and magneto-electric coefficients in their most general form represented by  $3 \times 3$  tensors. We will consider two numerical schemes for this formulation: with and without Lifeng Li's factorization rules. For both schemes, we provide explicit expressions for the Fourier tensors of macroscopic material parameters.

## II. CONVENTIONAL FOURIER MODAL METHOD

In this section, we will formulate basic ideas of the Fourier modal method in application to structures consisting of nonchiral reciprocal materials. We will also formulate Li's factorization rules, an approach that substantially enhances the convergence of the numerical scheme.

### A. Formulation

The principal sketch of a photonic structure to which the FMM can be applied is shown in Fig. 1. It consists of several layers, each of which is periodic along the horizontal plane and homogeneous along the vertical axis. The Maxwell's equations in such a system are solved using the formalism of a scattering matrix, which is based on finding the solution of an eigenvalue problem in each layer and subsequent connection of solutions of adjacent layers. In the following, we will use the Cartesian coordinate system, where the axes  $x^1$  and  $x^2$  form the periodicity plane, while the coordinate  $x^3$  corresponds to the direction along which the layers are homogeneous. Although the Fourier modal method is applicable to structures with arbitrary periodicity along the  $x^1 x^2$  plane, in this work we only consider a special case when the basis vectors of the unit cell coincide with the directions of orthogonal axes  $x^1$  and  $x^2$ .

Let us formulate the eigenvalue problem for a vertically homogeneous layer. Taking into account material equations for reciprocal nonchiral media in the form

$$\begin{cases} D^\rho = \epsilon^{\rho\sigma} E_\sigma, \\ B^\rho = \mu^{\rho\sigma} H_\sigma. \end{cases} \quad (1)$$

and assuming the time dependence as  $\exp(-i\omega t)$ , in the absence of electrical charges and currents, we can write Maxwell's equations in covariant form as

$$\begin{cases} \epsilon^{\rho\sigma\tau} \partial_\sigma E_\tau = ik_0 \mu^{\rho\sigma} H_\sigma, \\ \epsilon^{\rho\sigma\tau} \partial_\sigma H_\tau = -ik_0 \epsilon^{\rho\sigma} E_\sigma, \end{cases} \quad (2)$$

where  $E_\sigma$  and  $H_\sigma$  are components of electric and magnetic fields,  $\epsilon$  and  $\mu$  are macroscopic dielectric permittivity and magnetic permeability,  $k_0 = \omega/c$  is the absolute value of the wave vector. In periodic photonic structures,

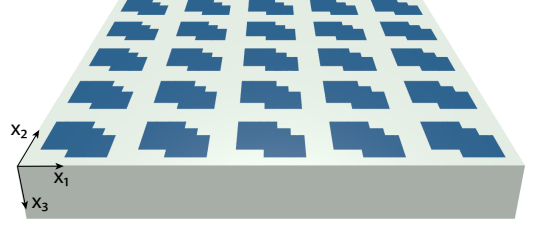


FIG. 1. Scheme of a two-dimensional photonic crystal slab. The colors indicate different materials.

$E_\sigma$  and  $H_\sigma$  satisfy Bloch's theorem:

$$\begin{aligned} E_\tau(x^1, x^2, x^3) &= \sum_{m=-G_1, n=-G_2}^{m=G_1, n=G_2} E_{\tau mn}(x^3) e^{ik_{1m}x^1 + ik_{2n}x^2}, \\ H_\tau(x^1, x^2, x^3) &= \sum_{m=-G_1, n=-G_2}^{m=G_1, n=G_2} H_{\tau mn}(x^3) e^{ik_{1m}x^1 + ik_{2n}x^2}, \end{aligned} \quad (3)$$

where  $\tau = 1, 2, 3$ ,  $m = 0, \pm 1, \pm 2, \dots, \pm G_1$ ,  $n = 0, \pm 1, \pm 2, \dots, \pm G_2$  and

$$\begin{aligned} k_{1m} &= k_{10} + m\Gamma_1, & \Gamma_1 &= \frac{2\pi}{a_1} \\ k_{2n} &= k_{20} + n\Gamma_2, & \Gamma_2 &= \frac{2\pi}{a_2} \end{aligned}$$

are two components of the Bloch vector, characterized by integer numbers  $m$  and  $n$ ,  $k_{10}$ , and  $k_{20}$  are components of the in-plane wave vector in the first Brillouin zone,  $a_1$  and  $a_2$  are the periods of the photonic structure along the  $x^1$  and  $x^2$  directions. Because the fields satisfy Bloch's theorem, we can introduce the Fourier space and characterize the fields by their Fourier components represented by vectors  $E_\tau$  and  $H_\tau$  with dimensionality  $N_g \times 1$  where  $N_g = (2G_1 + 1)(2G_2 + 1)$  is the number of Fourier harmonics. Based on this representation, Maxwell's equations (2) can be recast in the following form:

$$\begin{cases} k_{2n} E_{3mn} - \frac{\partial_3}{i} E_{2mn} = k_0 \sum_{p,q} \hat{\mu}_{mn,pq}^{1\sigma} H_{\sigma pq}, \\ \frac{\partial_3}{i} E_{1mn} - k_{1m} E_{3mn} = k_0 \sum_{p,q} \hat{\mu}_{mn,pq}^{2\sigma} H_{\sigma pq}, \\ k_{1m} E_{2mn} - k_{2n} E_{1mn} = k_0 \sum_{p,q} \hat{\mu}_{mn,pq}^{3\sigma} H_{\sigma pq}, \end{cases} \quad (4)$$

$$\begin{cases} k_{2n} H_{3mn} - \frac{\partial_3}{i} H_{2mn} = -k_0 \sum_{p,q} \hat{\epsilon}_{mn,pq}^{1\sigma} E_{\sigma pq}, \\ \frac{\partial_3}{i} H_{1mn} - k_{1m} H_{3mn} = -k_0 \sum_{p,q} \hat{\epsilon}_{mn,pq}^{2\sigma} E_{\sigma pq}, \\ k_{1m} H_{2mn} - k_{2n} H_{1mn} = -k_0 \sum_{p,q} \hat{\epsilon}_{mn,pq}^{3\sigma} E_{\sigma pq}. \end{cases} \quad (5)$$

Here,  $\hat{\epsilon}$ ,  $\hat{\mu}$  are the Toeplitz matrices,  $m$  and  $n$  are the row numbers,  $p$  and  $q$  are the column numbers, and  $\sigma$  is the convolution index. The Fourier representation  $\hat{\epsilon}$ ,  $\hat{\mu}$  can be expressed as

$$\hat{\epsilon} = F_1 F_2(\epsilon), \quad \hat{\mu} = F_1 F_2(\mu) \quad (6)$$

where  $F_\alpha$  is an operator that creates the matrices for products in Fourier space from the Fourier transform in direction  $x^\alpha$  using the Laurent's rule. Equations (4) and (5) are equivalent to (2) when  $G_{1,2} = \pm\infty$ .

Since the layer we are considering is vertically homogeneous, the fields and their Fourier components depend on the  $x^3$ -coordinate as  $\exp(ik_3x^3)$ . In this case, the partial derivative with respect to the  $x^3$ -coordinate gives the factor  $ik_3$ . Next, by introducing matrices

$$k_2 = k_{2n}\delta_{nq}\delta_{mp}, \quad k_1 = k_{1m}\delta_{nq}\delta_{mp}, \quad K_3 = k_{3mn}\delta_{nq}\delta_{mp},$$

and expressing  $E_3$  and  $H_3$  via the rest of the field components, we can write the eigenvalue problem for the vertically homogeneous layer as:

$$\mathbb{M}\mathbb{F} = K_3\mathbb{F}, \quad (7)$$

where  $\mathbb{F}$  is the  $4N_g \times 1$  column of the field Fourier amplitudes and  $\mathbb{M}$  is a master operator of the FMM represented by a  $4N_g \times 4N_g$  matrix of the second spatial derivatives in the Fourier space:

$$\mathbb{F} = \begin{pmatrix} E_1 \\ E_2 \\ H_1 \\ H_2 \end{pmatrix}, \quad \mathbb{M} = \begin{pmatrix} \mathbb{M}_{EE} & \mathbb{M}_{EH} \\ \mathbb{M}_{HE} & \mathbb{M}_{HH} \end{pmatrix}, \quad (8)$$

$$\begin{aligned} \mathbb{M}_{EE} &= \begin{pmatrix} -\tilde{\mu}_{23}k_2 - k_1\tilde{\varepsilon}_{31} & \tilde{\mu}_{23}k_1 - k_1\tilde{\varepsilon}_{32} \\ \tilde{\mu}_{13}k_2 - k_2\tilde{\varepsilon}_{31} & -\tilde{\mu}_{13}k_1 - k_2\tilde{\varepsilon}_{32} \end{pmatrix} \\ \mathbb{M}_{EH} &= \begin{pmatrix} k_0\tilde{\mu}_{21} + \frac{1}{k_0}k_1\tilde{\varepsilon}_{33}k_2 & k_0\tilde{\mu}_{22} - \frac{1}{k_0}k_1\tilde{\varepsilon}_{33}k_1 \\ -k_0\tilde{\mu}_{11} - \frac{1}{k_0}k_2\tilde{\varepsilon}_{33}k_2 & -k_0\tilde{\mu}_{12} - \frac{1}{k_0}k_2\tilde{\varepsilon}_{33}k_1 \end{pmatrix} \\ \mathbb{M}_{HE} &= \begin{pmatrix} -k_0\tilde{\varepsilon}_{21} - \frac{1}{k_0}k_1\tilde{\mu}_{33}k_2 & -k_0\tilde{\varepsilon}_{22} + \frac{1}{k_0}k_1\tilde{\mu}_{33}k_1 \\ k_0\tilde{\varepsilon}_{11} - \frac{1}{k_0}k_2\tilde{\mu}_{33}k_2 & k_0\tilde{\varepsilon}_{12} + \frac{1}{k_0}k_2\tilde{\mu}_{33}k_1 \end{pmatrix} \\ \mathbb{M}_{HH} &= \begin{pmatrix} -\tilde{\varepsilon}_{23}k_2 - k_1\tilde{\mu}_{31} & \tilde{\varepsilon}_{23}k_1 - k_1\tilde{\mu}_{32} \\ \tilde{\varepsilon}_{13}k_2 - k_2\tilde{\mu}_{31} & -\tilde{\varepsilon}_{13}k_1 - k_2\tilde{\mu}_{32} \end{pmatrix}. \end{aligned} \quad (9)$$

In these formulas,

$$\tilde{\varepsilon} \equiv l_3^-(\hat{\varepsilon}), \quad \tilde{\mu} \equiv l_3^-(\hat{\mu}) \quad (10)$$

where the operator  $l_3^-$  belongs to an operator class  $l_\tau^\pm$ , which when applied to a  $3 \times 3$  block matrix  $B = l_\tau^\pm A$ , gives the following result:

$$B^{\rho\sigma} = \begin{cases} (A^{\tau\tau})^{-1}, & \rho = \sigma = \tau \\ (A^{\tau\tau})^{-1} A^{\tau\sigma}, & \rho \neq \tau, \sigma = \tau \\ A^{\rho\tau} (A^{\tau\tau})^{-1}, & \rho = \tau, \sigma \neq \tau \\ A^{\rho\sigma} \pm A^{\rho\tau} (A^{\tau\tau})^{-1} A^{\tau\sigma}, & \rho \neq \tau, \sigma \neq \tau \end{cases} \quad (11)$$

The resulting field distribution in each layer is represented as a linear combination of eigen solutions of (7). The coefficients of this linear combination are found by solving the final scattering or eigenvalue problem written

in terms of the total scattering matrix with dimensionality  $4N_g \times 4N_g$ . The total scattering matrix is found as a sequence of Redheffer star products [18, 19] of the scattering matrices of layers and interfaces:

$$\mathbb{S}_{\text{total}} = \mathbb{S}_{N_s, N} \otimes \mathbb{S}_N \otimes \mathbb{S}_{N, N-1} \otimes \cdots \otimes \mathbb{S}_{21} \otimes \mathbb{S}_1 \otimes \mathbb{S}_{10}, \quad (12)$$

where  $N$  is the number of layers in a multilayered structure,  $\mathbb{S}_i$  is the scattering matrix of the  $i$ -th layer and  $\mathbb{S}_{ij}$  is the scattering matrix of the interface between the  $i$ -th and the  $j$ -th layer. These matrices can be found as

$$\mathbb{S}_n = \begin{pmatrix} e^{iK_3^{(n)}d_n} & 0 \\ 0 & e^{iK_3^{(n)}d_n} \end{pmatrix}, \quad (13)$$

$$\mathbb{S}_{n, n-1} = \Xi \{\mathbb{F}_n^{-1} \mathbb{F}_{n-1}\} \quad (14)$$

where  $\Xi$  is an operator that converts a transfer matrix into the scattering matrix [20],  $K_3^{(n)}$  is the diagonal matrix of eigenvalues  $k_3$  of the eigenvalue problem (7) in the  $n$ -th layer, and  $\mathbb{F}_n$  is the matrix of solutions of the eigenvalue problem (7) in the  $n$ -th layer.

The presented numerical scheme of finding the solution of Maxwell's equations in a layer and in the entire multilayered structure is subject to convergency check with respect to the number of Fourier harmonics. It is known that in periodic structures with high contrast of dielectric permittivity in the layer, the matrix elements in (8) may not converge quickly. Lifeng Li demonstrated [15–17] that to obtain better convergence, special rules should be used when calculating the operator  $\mathbb{M}$ .

## B. Li's factorization rules

The poor convergence in calculation of the matrix elements in  $\mathbb{M}$  originates mathematically from the Gibbs phenomenon that occurs when approximating a discontinuous function using a Fourier series. In application to Maxwell's equations, this problem starts at vertical material boundaries, where the macroscopic parameters such as dielectric permittivity undergo a jump discontinuity; so do the normal components of electromagnetic covariant vectors. As a result, the convolution of two functions with concurrent jump discontinuities hampers the convergence of the entire numerical scheme. The key point of Li's factorization rules involves using the most appropriate functions (direct or inverse) for the calculation of convolutions in matrix elements. As shown in [15], the positive effect for convergence is achieved when rewriting the eigenvalue problem in such a way that it does not contain products of two bounded, piecewise smooth periodic functions that have concurrent but not complementary jump discontinuities [15]. Using this strategy, one can significantly improve the convergence. The final scheme of factorization rules is expressed in terms of Eqn. (8) with the only difference that now the matrices

$\hat{\varepsilon}$  and  $\hat{\mu}$  are calculated using an improved scheme:

$$\hat{\varepsilon} = L_2 L_1(\varepsilon), \quad \hat{\mu} = L_2 L_1(\mu), \quad (15)$$

where

$$L_\tau = l_\tau^+ F_\tau l_\tau^- \quad (16)$$

with operators  $F_\tau$  and  $l_\tau^\pm$  defined above.

The material equation that describes the relationship between the electric induction and the electric field vectors after the Fourier transform can be represented using the aforementioned Li's operators:

$$D_{mn}^\rho = \sum_{p,q} \hat{\varepsilon}_{mn,pq}^{\rho\sigma} E_{\sigma pq}, \quad (17)$$

where  $\rho = 1, 2, 3$ , and  $\tau$  denote the direction under the Fourier transform.

The common feature of all schemes is that they are equivalent (except for rare special cases), meaning that they yield the same sum of series when taking an infinite number of Fourier harmonics. In practical realization, different schemes generally give different results even when using equal and large numbers of Fourier harmonics. The scheme set by the expression (6) is the simplest in terms of algebraic expressions, but converges slowly. An advanced scheme represented by (15) is more complex for practical implementation but demonstrates improved convergence. In addition to these, there exists a scheme, denoted as  $\hat{\varepsilon} = [(L_1 L_2(\varepsilon) + L_2 L_1(\varepsilon))/2]$ , which provides improved symmetry in solutions compared to scheme (15), although it sacrifices energy balance. In the implementation of the FMM, it is necessary to choose a scheme that is most suitable for a particular situation.

The authors in Refs. [15–17] demonstrated that applying factorization rules to the components of permittivity and permeability tensors enhances the convergence of the FMM numerical scheme. Yet, for further advancements, this method requires modifications when addressing materials that exhibit non-zero macroscopic magneto-electric coefficients.

### III. FOURIER MODAL METHOD FOR MAGNETO-ELECTRIC MEDIA

Extensive research on optical activity in the past century [10, 11, 21] can be summarized in the following constitutive relations, which are applicable to a general magneto-electric bi-anisotropic medium:

$$\begin{cases} D^\rho = \varepsilon^{\rho\sigma} E_\sigma + \chi^{\rho\sigma} H_\sigma, \\ B^\rho = \xi^{\rho\sigma} E_\sigma + \mu^{\rho\sigma} H_\sigma, \end{cases} \quad (18)$$

where  $\chi$  and  $\xi$  are local macroscopic magneto-electric tensors.

For the isotropic case, it can be shown that when  $\chi = -\xi$ , equations (18) describe a chiral reciprocal

medium. In the literature, this medium is referred to as a Pasteur medium, and  $i\chi$  carries the meaning of the chirality parameter, also known as a Pasteur parameter. A solution of randomly oriented chiral molecules with the same chirality is an example of the Pasteur medium. Conversely, the case of  $\chi = \xi$  corresponds to a non-chiral non-reciprocal medium termed a Tellegen medium, where  $\chi$  is known as a non-reciprocity parameter or Tellegen response. It should be noted that Tellegen media are much rarer than Pasteur medium, with only a limited number of realizations of the former being reported [22–25].

It should be kept in mind that the parameters  $\chi$  and  $\xi$  cannot take just any value; they are subject to constraints arising from the condition that the local energy dissipation rate must not be negative [26]. Specifically, for the dispersionless thermodynamically stable Pasteur medium, the chirality parameter is limited by  $|\text{Im}\{i\chi\}| \leq \sqrt{\text{Im}\{\varepsilon\}\text{Im}\{\mu\}}$ . While the real part of the chirality parameter  $i\chi$  is unrestricted, the medium's properties change significantly beyond the condition  $|i\chi| \leq \sqrt{\varepsilon\mu}$  [11]. For the dispersionless thermodynamically stable Tellegen medium, the non-reciprocity parameter must satisfy the condition  $|\chi| \leq \sqrt{\varepsilon\mu}$  [11, 26, 27]. In media with material resonances, the expression for the dissipation rate is modified, that eventually changes the above restrictions for the parameters [26].

In the following, we consider the most general magneto-electric bi-anisotropic media with arbitrary tensors  $\varepsilon$ ,  $\mu$ ,  $\chi$ , and  $\xi$ , assuming only that the local energy dissipation rate is not negative, and the medium is in thermodynamic equilibrium.

#### A. Eigenvalue problem for a layer with magneto-electric bi-anisotropic materials

Taking into account constitutive relations with non-zero parameters  $\chi^{\rho\sigma}$  and  $\xi^{\rho\sigma}$ , and using Fourier decomposition of the fields along the  $x^1$  and  $x^2$  directions in the form (3), we can write Maxwell's equations as a system of differential equations for the Fourier components of electric and magnetic fields:

$$\begin{cases} k_{2n} E_{3mn} - \frac{\partial_3}{i} E_{2mn} = k_0 \sum_{p,q} \hat{\varepsilon}_{mn,pq}^{1\sigma} E_{\sigma pq} + \hat{\mu}_{mn,pq}^{1\sigma} H_{\sigma pq}, \\ \frac{\partial_3}{i} E_{1mn} - k_{1m} E_{3mn} = k_0 \sum_{p,q} \hat{\varepsilon}_{mn,pq}^{2\sigma} E_{\sigma pq} + \hat{\mu}_{mn,pq}^{2\sigma} H_{\sigma pq}, \\ k_{1m} E_{2mn} - k_{2n} E_{1mn} = k_0 \sum_{p,q} \hat{\varepsilon}_{mn,pq}^{3\sigma} E_{\sigma pq} + \hat{\mu}_{mn,pq}^{3\sigma} H_{\sigma pq}, \end{cases} \quad (19)$$

$$\begin{cases} k_{2n} H_{3mn} - \frac{\partial_3}{i} H_{2mn} = -k_0 \sum_{p,q} \hat{\varepsilon}_{mn,pq}^{1\sigma} E_{\sigma pq} + \hat{\chi}_{mn,pq}^{1\sigma} H_{\sigma pq}, \\ \frac{\partial_3}{i} H_{1mn} - k_{1m} H_{3mn} = -k_0 \sum_{p,q} \hat{\varepsilon}_{mn,pq}^{2\sigma} E_{\sigma pq} + \hat{\chi}_{mn,pq}^{2\sigma} H_{\sigma pq}, \\ k_{1m} H_{2mn} - k_{2n} H_{1mn} = -k_0 \sum_{p,q} \hat{\varepsilon}_{mn,pq}^{3\sigma} E_{\sigma pq} + \hat{\chi}_{mn,pq}^{3\sigma} H_{\sigma pq}. \end{cases} \quad (20)$$

Next, by analogy with Sec. II, we extract  $E_3$  and  $H_3$  with the rest of the field components:

$$E_3 = \psi \varphi_{E_1}^{E_3} E_1 + \psi \varphi_{E_2}^{E_3} E_2 + \psi \varphi_{H_1}^{E_3} H_1 + \psi \varphi_{H_2}^{E_3} H_2, \quad (21)$$

$$H_3 = \varphi_{E_1}^{H_3} E_1 + \varphi_{E_2}^{H_3} E_2 + \varphi_{H_1}^{H_3} H_1 + \varphi_{H_2}^{H_3} H_2, \quad (22)$$

where

$$\begin{aligned} \psi &= \left( \hat{\varepsilon}^{33} - \hat{\xi}^{33} (\hat{\mu}^{33})^{-1} \hat{\xi}^{33} \right)^{-1}, \\ \varphi_{E_1}^{E_3} &= -\hat{\varepsilon}^{31} + \hat{\chi}^{33} (\hat{\mu}^{33})^{-1} \frac{k_2}{k_0} + \hat{\chi}^{33} (\hat{\mu}^{33})^{-1} \hat{\xi}^{31}, \\ \varphi_{E_2}^{E_3} &= -\hat{\varepsilon}^{32} - \hat{\chi}^{33} (\hat{\mu}^{33})^{-1} \frac{k_1}{k_0} + \hat{\chi}^{33} (\hat{\mu}^{33})^{-1} \hat{\xi}^{32}, \\ \varphi_{H_1}^{E_3} &= -\hat{\chi}^{31} + \hat{\chi}^{33} (\hat{\mu}^{33})^{-1} \hat{\mu}^{31} + \frac{k_2}{k_0}, \\ \varphi_{H_2}^{E_3} &= -\hat{\chi}^{32} + \hat{\chi}^{33} (\hat{\mu}^{33})^{-1} \hat{\mu}^{32} - \frac{k_1}{k_0}, \\ \varphi_{E_1}^{H_3} &= (\hat{\mu}^{33})^{-1} \left( -\frac{1}{k_0} k_2 - \hat{\xi}^{31} - \hat{\xi}^{33} \psi \varphi_{E_1}^{E_3} \right), \\ \varphi_{E_2}^{H_3} &= (\hat{\mu}^{33})^{-1} \left( \frac{1}{k_0} k_1 - \hat{\xi}^{32} - \hat{\xi}^{33} \psi \varphi_{E_2}^{E_3} \right), \\ \varphi_{H_1}^{H_3} &= (\hat{\mu}^{33})^{-1} \left( -\hat{\mu}^{31} - \hat{\xi}^{33} \psi \varphi_{H_1}^{E_3} \right), \\ \varphi_{H_2}^{H_3} &= (\hat{\mu}^{33})^{-1} \left( -\hat{\mu}^{32} - \hat{\xi}^{33} \psi \varphi_{H_2}^{E_3} \right). \end{aligned}$$

After substituting the field components  $E_3$  and  $H_3$  into the remaining four Maxwell's equations of systems (19)-(20), we obtain the master operator of the FMM

$$\mathbb{M} = \begin{pmatrix} \mathbb{M}_{11} & \mathbb{M}_{12} & \mathbb{M}_{13} & \mathbb{M}_{14} \\ \mathbb{M}_{21} & \mathbb{M}_{22} & \mathbb{M}_{23} & \mathbb{M}_{24} \\ \mathbb{M}_{31} & \mathbb{M}_{32} & \mathbb{M}_{33} & \mathbb{M}_{34} \\ \mathbb{M}_{41} & \mathbb{M}_{42} & \mathbb{M}_{43} & \mathbb{M}_{44} \end{pmatrix}, \quad (23)$$

with components

$$\begin{aligned} \mathbb{M}_{11} &= k_1 \psi \varphi_{E_1}^{E_3} + k_0 \hat{\xi}^{23} \psi \varphi_{E_1}^{E_3} + k_0 \hat{\mu}^{23} \varphi_{E_1}^{H_3} + k_0 \hat{\xi}^{21}, \\ \mathbb{M}_{12} &= k_1 \psi \varphi_{E_2}^{E_3} + k_0 \hat{\xi}^{23} \psi \varphi_{E_2}^{E_3} + k_0 \hat{\mu}^{23} \varphi_{E_2}^{H_3} + k_0 \hat{\xi}^{22}, \\ \mathbb{M}_{13} &= k_1 \psi \varphi_{H_1}^{E_3} + k_0 \hat{\xi}^{23} \psi \varphi_{H_1}^{E_3} + k_0 \hat{\mu}^{23} \varphi_{H_1}^{H_3} + k_0 \hat{\mu}^{21}, \\ \mathbb{M}_{14} &= k_1 \psi \varphi_{H_2}^{E_3} + k_0 \hat{\xi}^{23} \psi \varphi_{H_2}^{E_3} + k_0 \hat{\mu}^{23} \varphi_{H_2}^{H_3} + k_0 \hat{\mu}^{22}, \\ \mathbb{M}_{21} &= k_2 \psi \varphi_{E_1}^{E_3} - k_0 \hat{\xi}^{13} \psi \varphi_{E_1}^{E_3} - k_0 \hat{\mu}^{13} \varphi_{E_1}^{H_3} - k_0 \hat{\xi}^{11}, \\ \mathbb{M}_{22} &= k_2 \psi \varphi_{E_2}^{E_3} - k_0 \hat{\xi}^{13} \psi \varphi_{E_2}^{E_3} - k_0 \hat{\mu}^{13} \varphi_{E_2}^{H_3} - k_0 \hat{\xi}^{12}, \\ \mathbb{M}_{23} &= k_2 \psi \varphi_{H_1}^{E_3} - k_0 \hat{\xi}^{13} \psi \varphi_{H_1}^{E_3} - k_0 \hat{\mu}^{13} \varphi_{H_1}^{H_3} - k_0 \hat{\mu}^{11}, \\ \mathbb{M}_{24} &= k_2 \psi \varphi_{H_2}^{E_3} - k_0 \hat{\xi}^{13} \psi \varphi_{H_2}^{E_3} - k_0 \hat{\mu}^{13} \varphi_{H_2}^{H_3} - k_0 \hat{\mu}^{12}, \\ \mathbb{M}_{31} &= k_1 \varphi_{E_1}^{H_3} - k_0 \hat{\varepsilon}^{23} \psi \varphi_{E_1}^{E_3} - k_0 \hat{\chi}^{23} \varphi_{E_1}^{H_3} - k_0 \hat{\varepsilon}^{21}, \\ \mathbb{M}_{32} &= k_1 \varphi_{E_2}^{H_3} - k_0 \hat{\varepsilon}^{23} \psi \varphi_{E_2}^{E_3} - k_0 \hat{\chi}^{23} \varphi_{E_2}^{H_3} - k_0 \hat{\varepsilon}^{22}, \\ \mathbb{M}_{33} &= k_1 \varphi_{H_1}^{H_3} - k_0 \hat{\varepsilon}^{23} \psi \varphi_{H_1}^{E_3} - k_0 \hat{\chi}^{23} \varphi_{H_1}^{H_3} - k_0 \hat{\chi}^{21}, \\ \mathbb{M}_{34} &= k_1 \varphi_{H_2}^{H_3} - k_0 \hat{\varepsilon}^{23} \psi \varphi_{H_2}^{E_3} - k_0 \hat{\chi}^{23} \varphi_{H_2}^{H_3} - k_0 \hat{\chi}^{22}, \\ \mathbb{M}_{41} &= k_2 \varphi_{E_1}^{H_3} + k_0 \hat{\varepsilon}^{13} \psi \varphi_{E_1}^{E_3} + k_0 \hat{\chi}^{13} \varphi_{E_1}^{H_3} + k_0 \hat{\varepsilon}^{11}, \\ \mathbb{M}_{42} &= k_2 \varphi_{E_2}^{H_3} + k_0 \hat{\varepsilon}^{13} \psi \varphi_{E_2}^{E_3} + k_0 \hat{\chi}^{13} \varphi_{E_2}^{H_3} + k_0 \hat{\varepsilon}^{12}, \\ \mathbb{M}_{43} &= k_2 \varphi_{H_1}^{H_3} + k_0 \hat{\varepsilon}^{13} \psi \varphi_{H_1}^{E_3} + k_0 \hat{\chi}^{13} \varphi_{H_1}^{H_3} + k_0 \hat{\chi}^{11}, \\ \mathbb{M}_{44} &= k_2 \varphi_{H_2}^{H_3} + k_0 \hat{\varepsilon}^{13} \psi \varphi_{H_2}^{E_3} + k_0 \hat{\chi}^{13} \varphi_{H_2}^{H_3} + k_0 \hat{\chi}^{12}. \end{aligned} \quad (24)$$

which obviously reduce to (9) in the case of materials without magneto-electric coupling. In the following, we describe numerical schemes for calculating the matrices  $\hat{\varepsilon}$ ,  $\hat{\mu}$ ,  $\hat{\chi}$ , and  $\hat{\xi}$ .

## B. Numerical Schemes

Fourier representation of the parameters  $\varepsilon$ ,  $\mu$ ,  $\chi$ , and  $\xi$  can be obtained using different numerical schemes. We consider two numerical schemes for a grating with general bi-anisotropic materials. In the first scheme (referred to as Scheme 1), the expressions for the matrices  $\hat{\varepsilon}$ ,  $\hat{\mu}$ ,  $\hat{\chi}$ , and  $\hat{\xi}$  are obtained by taking the Fourier transform of the corresponding tensors independently using Laurent's rule:

$$\begin{aligned} \hat{\varepsilon} &= F_2 F_1(\varepsilon), \\ \hat{\chi} &= F_2 F_1(\chi), \\ \hat{\xi} &= F_2 F_1(\xi), \\ \hat{\mu} &= F_2 F_1(\mu) \end{aligned} \quad (25)$$

Scheme 1 does not employ factorization rules; it is represented in terms of already existing operators  $F_1$  and  $F_2$ , which makes its implementation quite straightforward.

Another scheme (Scheme 2) is formulated using factorization rules for all four tensors  $\varepsilon$ ,  $\chi$ ,  $\xi$ ,  $\mu$ . The Fourier representations of each of these parameters cannot be independently expressed using operators  $L_1$  and  $L_2$ . Instead, for the most general case of magneto-electric bi-anisotropic medium, each of the matrices  $\hat{\varepsilon}$ ,  $\hat{\mu}$ ,  $\hat{\chi}$ , and

$\hat{\xi}$  is a function of all the four dielectric parameters, and all these matrices are calculated simultaneously. This scheme can be illustrated with the following expression:

$$\begin{aligned}\hat{\varepsilon} &= S_{\varepsilon}(\varepsilon, \chi, \xi, \mu), \\ \hat{\chi} &= S_{\chi}(\varepsilon, \chi, \xi, \mu), \\ \hat{\xi} &= S_{\xi}(\varepsilon, \chi, \xi, \mu), \\ \hat{\mu} &= S_{\mu}(\varepsilon, \chi, \xi, \mu),\end{aligned}\tag{26}$$

where  $S_{\varepsilon, \chi, \xi, \mu}$  denotes the generalization of Li's operators  $L_{1,2}$ . The explicit form of the operator  $S$ , if it exists, is quite complicated. Because of this, instead of providing explicit expressions for operators  $S_{\varepsilon, \chi, \xi, \mu}$ , we present the algorithm to calculate the matrices  $\hat{\varepsilon}$ ,  $\hat{\mu}$ ,  $\hat{\chi}$ , and  $\hat{\xi}$  (see Appendices X, XI, XII).

From the explicit view of the  $\hat{\varepsilon}$ ,  $\hat{\chi}$ ,  $\hat{\xi}$ ,  $\hat{\mu}$  tensors, it follows that in the absence of the magneto-electric coupling, the operators  $S_{\varepsilon, \chi, \xi, \mu}$  reduce to the conventional Li's operators. To demonstrate this, we consider an expression for the tensor component  $\tilde{\varepsilon}^{21}$  (see Appendix XII)

$$\begin{aligned}\tilde{\varepsilon}^{21} &= [\varepsilon^{21} e_{E_1}^1 - \chi^{21} e_{H_1}^1] [(\varepsilon^{11})^{-1}]^{-1} + \\ &+ [-\varepsilon^{21} b_{E_1}^1 + \chi^{21} b_{H_1}^1] [(\xi^{11})^{-1}]^{-1},\end{aligned}\tag{27}$$

with coefficients

$$\begin{aligned}e_{H_1}^1 &= (\chi^{11} - \varepsilon^{11}(\xi^{11})^{-1}\mu^{11})^{-1}, \\ e_{E_1}^1 &= (\varepsilon^{11} - \chi^{11}(\mu^{11})^{-1}\xi^{11})^{-1}, \\ b_{H_1}^1 &= (\mu^{11} - \xi^{11}(\varepsilon^{11})^{-1}\chi^{11})^{-1}, \\ b_{E_1}^1 &= (\xi^{11} - \mu^{11}(\chi^{11})^{-1}\varepsilon^{11})^{-1}.\end{aligned}$$

In the absence of magneto-electric coupling, these coefficients reduce to

$$\begin{aligned}e_{H_1}^1 &= 0, & e_{E_1}^1 &= (\varepsilon^{11})^{-1}, \\ b_{H_1}^1 &= (\mu^{11})^{-1}, & b_{E_1}^1 &= 0.\end{aligned}$$

Substituting them into formula (27) we obtain

$$\tilde{\varepsilon}^{21} = [\varepsilon^{21} (\varepsilon^{11})^{-1}] [(\varepsilon^{11})^{-1}]^{-1}.$$

In the same way, one can obtain an expression for  $\tilde{\varepsilon}^{22}$  for the case without magneto-electric coupling:

$$\begin{aligned}\tilde{\varepsilon}^{22} &= [\varepsilon^{21} (\varepsilon^{11})^{-1}] [(\varepsilon^{11})^{-1}]^{-1} [(\varepsilon^{11}\varepsilon^{12})^{-1}] + \\ &+ [\varepsilon^{22} - \varepsilon^{21} (\varepsilon^{11})^{-1} \varepsilon^{12}].\end{aligned}$$

These expressions are nothing else but the elements 21 and 22 of the block matrix, which is the result of the action of the operator  $L_1$  on the tensor  $\varepsilon$

$$\tilde{\varepsilon} = L_1(\varepsilon),$$

where the Li's operator  $L_1$  is defined in (16). Next, by substituting the components  $\tilde{\varepsilon}^{21}$  and  $\tilde{\varepsilon}^{22}$  into the expression for  $\tilde{\varepsilon}^{21}$  (see Appendix XII) one can obtain the component  $\tilde{\varepsilon}^{21}(\chi = \xi = 0)$ , which appears to be equal to the element 21 of the block matrix  $\hat{\varepsilon}$  resulting from the action of the two operators  $L_1$  and  $L_2$  on the tensor  $\varepsilon$

$$\hat{\varepsilon} = L_2 L_1(\varepsilon).$$

By doing the same for the rest of the tensor components, it can easily be shown that in the case  $\chi = \xi = 0$

$$S_{\varepsilon, \chi, \xi, \mu}(\chi = \xi = 0) = L_2 L_1.$$

As previously mentioned, to develop correct factorization rules, one should construct the eigenvalue problem in a way that lacks products of two functions that have concurrent but non-complementary jump discontinuities (so-called type 3 product). From an algebraic perspective, type 3 products originate from material equations for the electric and magnetic induction vectors. To illustrate the Li's way of treatment of expressions with type 3 products, we consider the material equation for the  $D^1$  component written in the absence of bi-anisotropy, employing the Fourier transform in the  $x^1$  direction and assuming that all macroscopic material parameters have jump discontinuities

$$D^1 = \varepsilon^{11} E_1 + \varepsilon^{12} E_2 + \varepsilon^{13} E_3.\tag{28}$$

One can see that this expression contains the type 3 product in its first term  $\varepsilon^{11} E_1$ . Because of this, an eigenvalue problem constructed from Maxwell's equation by replacing the  $D^1$  term with the right-hand side of Eq. (IIIB) would demonstrate poor convergence. To overcome this problem, Li offered rewriting expression in the form

$$D^1 = \varepsilon^{11} (E_1 + (\varepsilon^{11})^{-1} \varepsilon^{12} E_2 + (\varepsilon^{11})^{-1} \varepsilon^{13} E_3),\tag{29}$$

which obviously does not contain type 3 products. In the presence of the chiral coefficients, the same material equation takes the form

$$D^1 = \varepsilon^{11} E_1 + \varepsilon^{12} E_2 + \varepsilon^{13} E_3 + \chi^{11} H_1 + \chi^{12} H_2 + \chi^{13} H_3\tag{30}$$

We try to avoid that "bad" type of product in the same way

$$\begin{aligned}D^1 &= \varepsilon^{11} (E_1 + (\varepsilon^{11})^{-1} \varepsilon^{12} E_2 + (\varepsilon^{11})^{-1} \varepsilon^{13} E_3) + \\ &+ \chi^{11} (H_1 + (\chi^{11})^{-1} \chi^{12} H_2 + (\chi^{11})^{-1} \chi^{13} H_3).\end{aligned}\tag{31}$$

Since the normal component of electric induction vector is continuous in all media, including bi-anisotropic ones, both sides of Eq. (31) are continuous functions.

For the implementation of Scheme 2, we assume that not only is the right-hand side of Eq. (31) (and similar equations for the remaining components  $D^\sigma$  and  $B^\sigma$  with type 3 products) continuous, but also that both terms

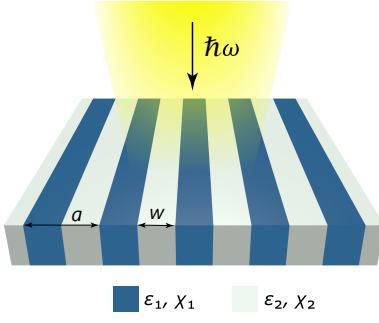


FIG. 2. One-dimensional grating for the demonstration of convergence. The colors indicate different materials.

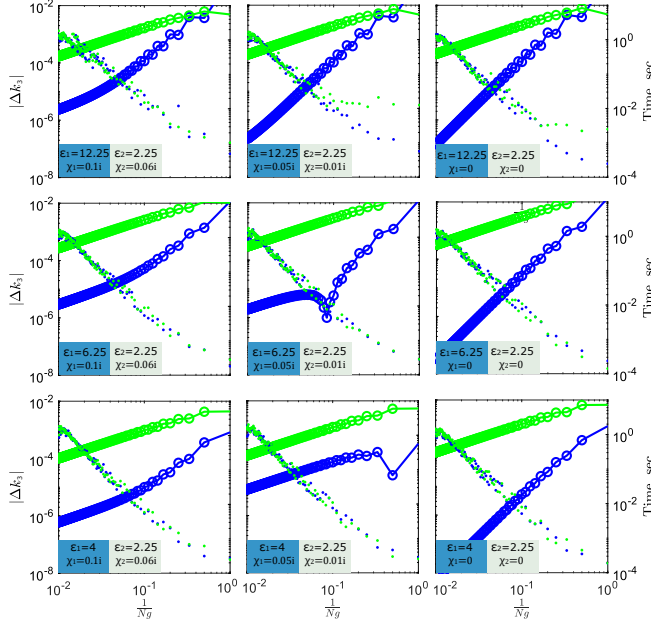


FIG. 3. Convergence of the two numerical schemes to the analytical solution in a double logarithmic scale for different values of the refractive indices and chirality coefficients. The green and blue curves represent Scheme 1 (without factorization rules) and Scheme 2 (with factorization rules), respectively.  $|\Delta k_z|$  denotes the difference between the  $k_z$  value calculated by numerical Schemes 1 and 2 and the exact value, obtained analytically. The computation time for the main matrix  $\mathbb{M}$  is shown by the blue and green dots for each number of harmonics.  $\hbar\omega = 1320$  meV,  $k_1 = k_2 = 0$ . For calculations, we used a 14-core 12th Gen Intel(R) Core(TM) i7-12700H processor, with 16 GB of RAM.

of it are continuous. Although strictly speaking this is not true, such an assumption can be fulfilled with the required accuracy, since the values of the bi-anisotropy coefficients are usually small. In the following section, we will show that, despite the fact that the continuity of both terms of the right-hand side of Eq. (31) is only an assumption, the improved numerical scheme (Scheme 2) offers better convergence compared to the scheme without factorization rules (Scheme 1). This holds true even

when the values of the chiral coefficients are on the order of  $10^{-1}$ .

#### IV. CONVERGENCE COMPARISON

To illustrate the convergence of the considered numerical schemes, we use the example of a one-dimensional photonic crystal slab shown in Fig. 2. The structure consists of alternating stripes of two different materials with a period of  $a = 500$  nm. We consider the materials to be isotropic and reciprocal, so that  $\xi$  and  $\chi$  are scalars and  $\xi = -\chi$ . In the following, we consider different pairs of  $\varepsilon$  and  $\chi$  to see the impact of the material contrast on the convergence (see Fig. 3). Calculations are made for the photon energy  $\hbar\omega = 1320$  meV and the zero in-plane wavevector ( $k_1 = k_2 = 0$ ).

To investigate the convergence of numerical schemes, for each number of Fourier harmonics  $N_g$  in the range between 1 and 100, we solve eigenvalue problem (7), where the matrix  $\mathbb{M}$  is calculated either by Scheme 1 or Scheme 2. Then, from each solution we find such eigenvalue  $k_3$  in the diagonal matrix  $K_3$  that  $\text{Re}(k_z)$  has the highest value and compare this approximate quantity with the exact solution obtained analytically (see Appendix VIII for details on finding the exact value of  $k_3$ ).

In Fig. 3, we plot the absolute value of the deviation of the approximate  $k_3$  from the exact  $k_3$ ,  $|\Delta k_3|$ , as a function of the number of Fourier harmonics  $N_g$ . One can see from Fig. 3 that in the considered range of  $N_g$ , in all graphs, the deviation  $|\Delta k_3|$  decreases as  $N_g^{-p}$ , where  $p = 1$  for Scheme 1 and varies between 1 and 3 for Scheme 2. One can also observe that for all pairs  $n$  and  $\chi$  Scheme 2 converges faster than Scheme 1.

In Fig. 3, we also plot the computation time required to solve the eigenvalue problem (7) as a function of the number of Fourier harmonics,  $N_g$ . This time represents the total duration for the numerical solver to compute the eigenvalues for a given matrix size  $4N_g \times 4N_g$ . As one can see from the resulting curve, in the considered range of  $N_g$  the computation time scales with the square of the number of Fourier harmonics (that is,  $t \propto N_g^2$ ).

#### V. NUMERICAL EXAMPLE

As a numerical demonstration, we consider a metasurface consisting of a square lattice of geometrically chiral elements embedded in a matrix. The structure is located on an  $\text{SiO}_2$  substrate ( $\varepsilon_s = 2.25$ ) and is surrounded by air from the top, as shown in Fig. 4a. The lattice has a period of  $a = 500$  nm and a layer height of  $h = 220$  nm. The blue elements in Fig. 4a correspond to an isotropic reciprocal chiral material with the parameters  $\varepsilon = 12.25 + 0.01i$ ,  $\mu = 1$  and  $\chi = \xi = \pm 0.1i$ , while the grey elements denote a non-chiral, isotropic reciprocal material characterized by  $\varepsilon_m = 2.25 + 0.01i$ ,  $\mu = 1$

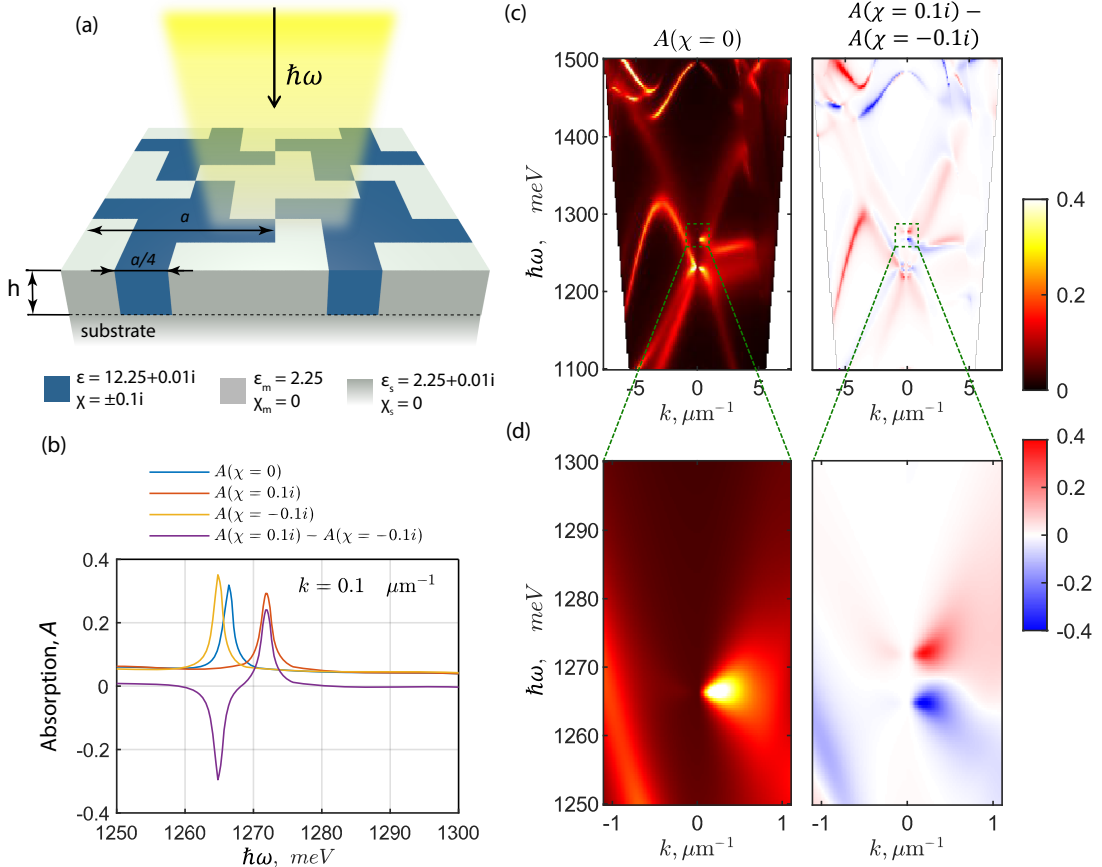


FIG. 4. (a) Schematic illustration of the metasurface, comprising a periodic array of chiral elements on a substrate. The blue and grey colors represent materials with distinct dielectric permittivities  $\epsilon$  and chirality parameters  $\chi$  (b) Absorption spectra calculated in  $p$ -polarization at  $k_1 = 0.1 \mu\text{m}^{-1}$ . (c) and (d) left panels — Photon energy and in-plane wavevector dependencies of the absorption coefficient calculated for the non-chiral case with  $\chi = \xi^* = 0$ . (c) and (d) right panels — The difference of the absorption spectra calculated for different signs of chiral coefficients. In (c) and (d) the positive and negative values of  $k$  correspond to the  $\Gamma - X$  and  $\Gamma - M$  directions in reciprocal space. The calculation was performed by selecting 11 harmonics by  $x$  direction and 11 harmonics by  $y$  direction.

and  $\chi = \xi = 0$ .

Using Scheme 2, we calculate the absorption spectra for incident  $p$ -polarized light. Figure 4b presents the absorption at a fixed in-plane wavevector ( $k_1 = 0.1 \mu\text{m}^{-1}$ ) for both chiral ( $\chi = \pm 0.1i$ ) and non-chiral ( $\chi = 0$ ) cases along with their difference. The spectra exhibit pronounced peaks corresponding to guided resonant modes (also known as quasiguided modes). One can see that introducing chirality shifts the peak position, resulting in a redshift or blueshift relative to the non-chiral case that depends on the sign of the macroscopic chirality coefficient  $\chi$ .

The dependence of the absorption coefficient on both the photon energy and in-plane wavevector is shown for the non-chiral case ( $\chi = -\xi = 0$ ) in Fig. 4c,d. The right panels display the difference in absorption between the two opposite chiralities. This differential map, with red (positive) and blue (negative) colors, clearly reveals the slight energy shift of the resonant modes induced by non-zero chirality.

## VI. CONCLUSION

In conclusion, we have developed a comprehensive and advanced formulation of the Fourier modal method tailored for the rigorous analysis of two-dimensionally periodic multilayered structures composed of magneto-electric bi-anisotropic materials characterized by macroscopic complex-valued coefficients  $\epsilon$ ,  $\mu$ ,  $\xi$  and  $\chi$ . Our work generalizes the conventional FMM framework by incorporating arbitrary  $3 \times 3$  tensors for the macroscopic magneto-electric coefficients, thereby enabling the study of a vast range of periodic structures with chiral and non-reciprocal materials. An important feature of this study is the detailed comparison of two numerical schemes: one implementing generalized Lifeng Li's factorization rules and one without. We have derived explicit expressions for the Fourier tensors in both cases, demonstrating their correct reduction to established forms in the limit of absence of magneto-electric coupling. Crucially, our analysis confirms that the application of factorization rules



remains essential, as this scheme delivers superior convergence rates even for structures exhibiting large macroscopic chirality. Therefore, this enhanced formulation establishes itself as a fast, rigorous, and versatile computational technique for the design and theoretical investigation of next-generation photonic devices leveraging the full potential of advanced chiral and bi-anisotropic materials.

## VII. ACKNOWLEDGEMENT

This work was supported by the Russian Science Foundation (project 25-12-00454). S.D. acknowledges Maxim Gorchak for a fruitful discussion.

## VIII. APPENDIX A. ANALYTICAL SOLUTION IN A SLAB WITH ONE-DIMENSIONAL PERIODICITY

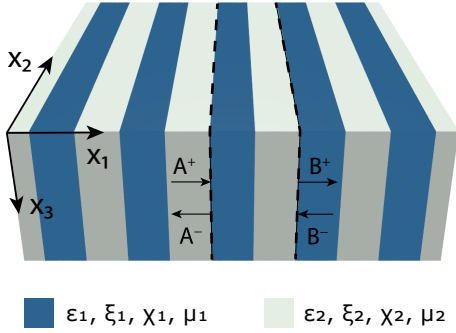


FIG. 5. Finding an exact value of  $k_3$  in a slab with one-dimensional periodicity. Dashed lines denote boundaries of the considered unit cell.

To find the exact solution in a periodic slab with one-dimensional periodicity, one can look at it from a different perspective, considering that our slab is a multilayered stratified medium with all layers being homogeneous and infinite in lateral directions. Since we are only interested in finding the exact value  $k_3$  in the slab, we do not use its thickness as an input parameter for our problem, nor do we need any information on the adjacent layers. Hence, despite the fact that in the FMM all layers (except for the substrate and superstrate) are characterized by a certain thickness, these two representations are fully equivalent for our purpose. Due to homogeneity of the layers in a stratified system, Maxwell's equations in it can be solved analytically. One of the ways of doing so is using the scattering-matrix formalism, a well established technique for such types of media, since it does not require Fourier transform [28].

In order to find the exact value  $k_3$  of modes (plane waves) propagating in the stratified medium with an infinite number of periods, we write the definition of the

scattering matrix  $\mathbb{S}$  connecting incoming and outgoing amplitudes for one period, as shown in Fig. 5:

$$\mathbb{S}(\omega, k_3) \begin{pmatrix} A^+ \\ B^- \end{pmatrix} = \begin{pmatrix} B^+ \\ A^- \end{pmatrix},$$

where  $A^\pm$  and  $B^\pm$  are the amplitudes of plane waves propagating in the positive and negative  $x_1$  directions in the stratified periodic medium, and  $k_3$  now plays a role of the problem parameter, along with  $\omega$ . Then, applying Bloch's theorem to the mode's field,

$$B^+ = A^+ e^{ik_1 x_1}, \quad A^- = B^- e^{-ik_1 x_1},$$

we find that plane waves propagating in the stratified periodic medium and characterizing by the photon energy  $\omega$  and wavevector  $(k_1, 0, k_3)$  must satisfy the following equation:

$$\begin{pmatrix} e^{-ik_1 x_1} & 0 \\ 0 & e^{ik_1 x_1} \end{pmatrix} \mathbb{S}(\omega, k_3) \begin{pmatrix} A^+ \\ B^- \end{pmatrix} = \begin{pmatrix} A^+ \\ B^- \end{pmatrix}.$$

Therefore, in order to find the exact value  $k_3$  of the modes in the initial periodic slab with one-dimensional periodicity, one should vary  $k_3$  as an independent parameter at fixed  $\omega$  and  $k_1$ , to obtain the matrix  $\mathbb{C}$

$$\mathbb{C}(\omega, k_1, k_3) = \begin{pmatrix} e^{-ik_1 x_1} & 0 \\ 0 & e^{ik_1 x_1} \end{pmatrix} \mathbb{S}(\omega, k_3) \quad (32)$$

such that one of its eigenvalues equals 1. The procedure will provide us with the exact (analytical) value of  $k_3$ , accurate to machine precision.

## IX. APPENDIX B. MASTER OPERATOR OF THE FMM FOR MAGNETO-ELECTRIC BI-ANISOTROPIC MATERIALS

This section details the derivation of the matrix  $\mathbb{M}$  (Eq. (23)). Beginning with the first equation of the system (19)

$$k_{2n} E_{3mn} - \frac{\partial_3}{i} E_{2mn} = k_0 \sum_{p,q} \hat{\xi}_{mn,pq}^{1\sigma} E_{\sigma pq} + \hat{\mu}_{mn,pq}^{1\sigma} H_{\sigma pq},$$

the field component  $H_3$  is expressed as

$$H_3 = (\hat{\mu}^{33})^{-1} (\hat{\mu}^{33})^{-1} \left( \frac{1}{k_0} (k_1 E_2 - k_2 E_1) - \hat{\xi}^{3\sigma} E_\sigma - \hat{\mu}^{31} H_1 - \hat{\mu}^{32} H_2 \right). \quad (33)$$

This expression is then substituted into the first equation of system (20)

$$k_{2n}H_{3mn} - \frac{\partial_3}{i}H_{2mn} = -k_0 \sum_{p,q} \hat{\varepsilon}_{mn,pq}^{1\sigma} E_{\sigma pq} + \hat{\chi}_{mn,pq}^{1\sigma} H_{\sigma pq},$$

yielding the field component  $E_3$  as a linear combination of the remaining field components  $E_3 = E_3(E_1, E_2, H_1, H_2)$ . After algebraic manipulations, the field component  $E_3$  acquires the following form:

$$E_3 = \psi \varphi_{E_1}^{E_3} E_1 + \psi \varphi_{E_2}^{E_3} E_2 + \psi \varphi_{H_1}^{E_3} H_1 + \psi \varphi_{H_2}^{E_3} H_2 \quad (34)$$

with coefficients

$$\begin{aligned} \psi &= \left( \hat{\varepsilon}^{33} - \hat{\xi}^{33} (\hat{\mu}^{33})^{-1} \hat{\xi}^{33} \right)^{-1}, \\ \varphi_{E_1}^{E_3} &= -\hat{\varepsilon}^{31} + \hat{\chi}^{33} (\hat{\mu}^{33})^{-1} \frac{k_2}{k_0} + \hat{\chi}^{33} (\hat{\mu}^{33})^{-1} \hat{\xi}^{31}, \\ \varphi_{E_2}^{E_3} &= -\hat{\varepsilon}^{32} - \hat{\chi}^{33} (\hat{\mu}^{33})^{-1} \frac{k_1}{k_0} + \hat{\chi}^{33} (\hat{\mu}^{33})^{-1} \hat{\xi}^{32}, \\ \varphi_{H_1}^{E_3} &= -\hat{\chi}^{31} + \hat{\chi}^{33} (\hat{\mu}^{33})^{-1} \hat{\mu}^{31} + \frac{k_2}{k_0}, \\ \varphi_{H_2}^{E_3} &= -\hat{\chi}^{32} + \hat{\chi}^{33} (\hat{\mu}^{33})^{-1} \hat{\mu}^{32} - \frac{k_1}{k_0}. \end{aligned}$$

Substituting the result for  $E_3$  (34) into the expression for  $H_3$  (33), we obtain the  $H_3$  as a linear combination of the remaining field components  $H_3 = H_3(E_1, E_2, H_1, H_2)$

$$H_3 = \varphi_{E_1}^{H_3} E_1 + \varphi_{E_2}^{H_3} E_2 + \varphi_{H_1}^{H_3} H_1 + \varphi_{H_2}^{H_3} H_2 \quad (35)$$

with the following coefficients

$$\begin{aligned} \varphi_{E_1}^{H_3} &= (\hat{\mu}^{33})^{-1} \left( -\frac{1}{k_0} k_2 - \hat{\xi}^{31} - \hat{\xi}^{33} \psi \varphi_{E_1}^{E_3} \right), \\ \varphi_{E_2}^{H_3} &= (\hat{\mu}^{33})^{-1} \left( \frac{1}{k_0} k_1 - \hat{\xi}^{32} - \hat{\xi}^{33} \psi \varphi_{E_2}^{E_3} \right), \\ \varphi_{H_1}^{H_3} &= (\hat{\mu}^{33})^{-1} \left( -\hat{\mu}^{31} - \hat{\xi}^{33} \psi \varphi_{H_1}^{E_3} \right), \\ \varphi_{H_2}^{H_3} &= (\hat{\mu}^{33})^{-1} \left( -\hat{\mu}^{32} - \hat{\xi}^{33} \psi \varphi_{H_2}^{E_3} \right). \end{aligned}$$

At this stage, the field components  $E_3$  and  $H_3$  are known. We now substitute them into the remaining four vector Maxwell's equations from systems (19), (20). As an example, the substitution into the first of these equations

yields

$$\begin{aligned} &\left( \frac{k_2}{k_0} \psi \varphi_{E_1}^{E_3} - \hat{\xi}^{11} - \hat{\xi}^{13} \psi \varphi_{E_1}^{E_3} - \hat{\mu}^{13} \varphi_{E_1}^{H_3} \right) E_1 + \\ &+ \left( \frac{k_2}{k_0} \psi \varphi_{E_2}^{E_3} - \hat{\xi}^{12} - \hat{\xi}^{13} \psi \varphi_{E_2}^{E_3} - \hat{\mu}^{13} \varphi_{E_2}^{H_3} \right) E_2 + \\ &+ \left( \frac{k_2}{k_0} \psi \varphi_{H_1}^{E_3} - \hat{\mu}^{11} - \hat{\xi}^{13} \psi \varphi_{H_1}^{E_3} - \hat{\mu}^{13} \varphi_{H_1}^{H_3} \right) H_1 + \\ &+ \left( \frac{k_2}{k_0} \psi \varphi_{H_2}^{E_3} - \hat{\mu}^{12} - \hat{\xi}^{13} \psi \varphi_{H_2}^{E_3} - \hat{\mu}^{13} \varphi_{H_2}^{H_3} \right) H_2 = \frac{K_3}{k_0} E_2. \end{aligned}$$

Since the eigenvalue  $K_3$  on the right-hand side is associated with the component  $E_2$ , we obtain the second row of the matrix  $\mathbb{M}$  (with all terms multiplied by  $k_0$ )

$$\begin{aligned} \mathbb{M}_{21} &= k_2 \psi \varphi_{E_1}^{E_3} - k_0 \hat{\xi}^{13} \psi \varphi_{E_1}^{E_3} - k_0 \hat{\mu}^{13} \varphi_{E_1}^{H_3} - k_0 \hat{\xi}^{11}, \\ \mathbb{M}_{22} &= k_2 \psi \varphi_{E_2}^{E_3} - k_0 \hat{\xi}^{13} \psi \varphi_{E_2}^{E_3} - k_0 \hat{\mu}^{13} \varphi_{E_2}^{H_3} - k_0 \hat{\xi}^{12}, \\ \mathbb{M}_{23} &= k_2 \psi \varphi_{H_1}^{E_3} - k_0 \hat{\xi}^{13} \psi \varphi_{H_1}^{E_3} - k_0 \hat{\mu}^{13} \varphi_{H_1}^{H_3} - k_0 \hat{\mu}^{11}, \\ \mathbb{M}_{24} &= k_2 \psi \varphi_{H_2}^{E_3} - k_0 \hat{\xi}^{13} \psi \varphi_{H_2}^{E_3} - k_0 \hat{\mu}^{13} \varphi_{H_2}^{H_3} - k_0 \hat{\mu}^{12}. \end{aligned}$$

The full form of matrix  $\mathbb{M}$  is obtained straightforwardly by applying the same procedure:

$$\begin{aligned} \mathbb{M}_{11} &= k_1 \psi \varphi_{E_1}^{E_3} + k_0 \hat{\xi}^{23} \psi \varphi_{E_1}^{E_3} + k_0 \hat{\mu}^{23} \varphi_{E_1}^{H_3} + k_0 \hat{\xi}^{21}, \\ \mathbb{M}_{12} &= k_1 \psi \varphi_{E_2}^{E_3} + k_0 \hat{\xi}^{23} \psi \varphi_{E_2}^{E_3} + k_0 \hat{\mu}^{23} \varphi_{E_2}^{H_3} + k_0 \hat{\xi}^{22}, \\ \mathbb{M}_{13} &= k_1 \psi \varphi_{H_1}^{E_3} + k_0 \hat{\xi}^{23} \psi \varphi_{H_1}^{E_3} + k_0 \hat{\mu}^{23} \varphi_{H_1}^{H_3} + k_0 \hat{\mu}^{21}, \\ \mathbb{M}_{14} &= k_1 \psi \varphi_{H_2}^{E_3} + k_0 \hat{\xi}^{23} \psi \varphi_{H_2}^{E_3} + k_0 \hat{\mu}^{23} \varphi_{H_2}^{H_3} + k_0 \hat{\mu}^{22}, \\ \mathbb{M}_{31} &= k_1 \varphi_{E_1}^{H_3} - k_0 \hat{\varepsilon}^{23} \psi \varphi_{E_1}^{E_3} - k_0 \hat{\chi}^{23} \varphi_{E_1}^{H_3} - k_0 \hat{\varepsilon}^{21}, \\ \mathbb{M}_{32} &= k_1 \varphi_{E_2}^{H_3} - k_0 \hat{\varepsilon}^{23} \psi \varphi_{E_2}^{E_3} - k_0 \hat{\chi}^{23} \varphi_{E_2}^{H_3} - k_0 \hat{\varepsilon}^{22}, \\ \mathbb{M}_{33} &= k_1 \varphi_{H_1}^{H_3} - k_0 \hat{\varepsilon}^{23} \psi \varphi_{H_1}^{E_3} - k_0 \hat{\chi}^{23} \varphi_{H_1}^{H_3} - k_0 \hat{\chi}^{21}, \\ \mathbb{M}_{34} &= k_1 \varphi_{H_2}^{H_3} - k_0 \hat{\varepsilon}^{23} \psi \varphi_{H_2}^{E_3} - k_0 \hat{\chi}^{23} \varphi_{H_2}^{H_3} - k_0 \hat{\chi}^{22}, \\ \mathbb{M}_{41} &= k_2 \varphi_{E_1}^{H_3} + k_0 \hat{\varepsilon}^{13} \psi \varphi_{E_1}^{E_3} + k_0 \hat{\chi}^{13} \varphi_{E_1}^{H_3} + k_0 \hat{\varepsilon}^{11}, \\ \mathbb{M}_{42} &= k_2 \varphi_{E_2}^{H_3} + k_0 \hat{\varepsilon}^{13} \psi \varphi_{E_2}^{E_3} + k_0 \hat{\chi}^{13} \varphi_{E_2}^{H_3} + k_0 \hat{\varepsilon}^{12}, \\ \mathbb{M}_{43} &= k_2 \varphi_{H_1}^{H_3} + k_0 \hat{\varepsilon}^{13} \psi \varphi_{H_1}^{E_3} + k_0 \hat{\chi}^{13} \varphi_{H_1}^{H_3} + k_0 \hat{\chi}^{11}, \\ \mathbb{M}_{44} &= k_2 \varphi_{H_2}^{H_3} + k_0 \hat{\varepsilon}^{13} \psi \varphi_{H_2}^{E_3} + k_0 \hat{\chi}^{13} \varphi_{H_2}^{H_3} + k_0 \hat{\chi}^{12}. \end{aligned}$$

We therefore have assembled the master operator of the Fourier modal method  $\mathbb{M}$

$$\mathbb{M} = \begin{pmatrix} \mathbb{M}_{11} & \mathbb{M}_{12} & \mathbb{M}_{13} & \mathbb{M}_{14} \\ \mathbb{M}_{21} & \mathbb{M}_{22} & \mathbb{M}_{23} & \mathbb{M}_{24} \\ \mathbb{M}_{31} & \mathbb{M}_{32} & \mathbb{M}_{33} & \mathbb{M}_{34} \\ \mathbb{M}_{41} & \mathbb{M}_{42} & \mathbb{M}_{43} & \mathbb{M}_{44} \end{pmatrix}.$$

## X. APPENDIX C. FOURIER TRANSFORM IN $x^1$

In this section, we derive the Fourier transform along the  $x^1$ -direction. Equivalently, our goal is to find the

matrix  $\tilde{Q}$  such that

$$\begin{pmatrix} D^1(k^1, x^2) \\ B^1(k^1, x^2) \end{pmatrix} = \tilde{Q} \begin{pmatrix} E_1(k^1, x^2) \\ H_1(k^1, x^2) \end{pmatrix}. \quad (36)$$

Following Li's paradigm [15], we have to avoid the so-called type 3 products  $h = f \cdot g$ , which arises when functions  $f$  and  $g$  have concurrent non-complementary jump discontinuities. Here  $h, f, g \in P$ , where  $P$  denotes the set of piecewise-continuous piecewise-smooth bounded periodic functions. Since we need to perform the Fourier transform along the  $x^1$ -axis, we begin with the material equations for the case  $\rho = 1$

$$\begin{cases} D^1 = \varepsilon^{1\sigma} E_\sigma + \chi^{1\sigma} H_\sigma, \\ B^1 = \xi^{1\sigma} E_\sigma + \mu^{1\sigma} H_\sigma. \end{cases} \quad (37)$$

From the first equation of system (37), we express the field component  $E_1$ , then substitute it into the second equation of system (37), and thereby express the component  $H_1$  via  $D^1$ ,  $E_2$ ,  $E_3$ ,  $B^1$ ,  $H_2$ , and  $H_3$ :

$$\begin{aligned} H_1 = & (\mu^{11} - \xi^{11}(\varepsilon^{11})^{-1}\chi^{11})^{-1} \left[ -\xi^{11}(\varepsilon^{11})^{-1}D^1 - \right. \\ & - (\xi^{12} - \xi^{11}(\varepsilon^{11})^{-1}\varepsilon^{12}) E_2 - (\xi^{13} - \xi^{11}(\varepsilon^{11})^{-1}\varepsilon^{13}) E_3 + \\ & + B^1 - (\mu^{12} - \xi^{11}(\varepsilon^{11})^{-1}\chi^{12}) H_2 - \\ & \left. - (\mu^{13} - \xi^{11}(\varepsilon^{11})^{-1}\chi^{13}) H_3 \right]. \end{aligned}$$

From the second equation of system (37) we express the field component  $H_1$ , and substitute the result into the first equation of system (37), thereby expressing the field component  $E_1$  via  $D^1$ ,  $E_2$ ,  $E_3$ ,  $B^1$ ,  $H_2$ , and  $H_3$

$$\begin{aligned} E_1 = & (\varepsilon^{11} - \chi^{11}(\mu^{11})^{-1}\xi^{11})^{-1} \left[ D^1 - \right. \\ & - (\varepsilon^{12} - \chi^{11}(\mu^{11})^{-1}\xi^{12}) E_2 - (\varepsilon^{13} - \chi^{11}(\mu^{11})^{-1}\xi^{13}) E_3 - \\ & - \chi^{11}(\mu^{11})^{-1}B^1 - (\chi^{12} - \chi^{11}(\mu^{11})^{-1}\mu^{12}) H_2 - \\ & \left. - (\chi^{13} - \chi^{11}(\mu^{11})^{-1}\mu^{13}) H_3 \right]. \end{aligned}$$

Briefly,  $E_1$  and  $H_1$  can be represented as

$$\begin{aligned} H_1 = & -e_{H_1}^1 D^1 - e_{H_1}^2 E_2 - e_{H_1}^3 E_3 + b_{H_1}^1 B^1 - b_{H_1}^2 H_2 - b_{H_1}^3 H_3, \\ E_1 = & e_{E_1}^1 D^1 - e_{E_1}^2 E_2 - e_{E_1}^3 E_3 - b_{E_1}^1 B^1 - b_{E_1}^2 H_2 - b_{E_1}^3 H_3. \end{aligned}$$

where new symbols are introduced

$$\begin{aligned} e_{H_1}^1 &= K_2 \xi^{11} (\varepsilon^{11})^{-1} = -K_3, \\ e_{H_1}^2 &= K_2 (\xi^{12} - \xi^{11} (\varepsilon^{11})^{-1} \varepsilon^{12}), \\ e_{H_1}^3 &= K_2 (\xi^{13} - \xi^{11} (\varepsilon^{11})^{-1} \varepsilon^{13}), \\ b_{H_1}^1 &= K_2, \\ b_{H_1}^2 &= K_2 (\mu^{12} - \xi^{11} (\varepsilon^{11})^{-1} \chi^{12}), \\ b_{H_1}^3 &= K_2 (\mu^{13} - \xi^{11} (\varepsilon^{11})^{-1} \chi^{13}), \\ e_{E_1}^1 &= K_1, \\ e_{E_1}^2 &= K_1 (\varepsilon^{12} - \chi^{11} (\mu^{11})^{-1} \xi^{12}), \\ e_{E_1}^3 &= K_1 (\varepsilon^{13} - \chi^{11} (\mu^{11})^{-1} \xi^{13}), \\ b_{E_1}^1 &= K_1 \chi^{11} (\mu^{11})^{-1} = -K_4, \\ b_{E_1}^2 &= K_1 (\chi^{12} - \chi^{11} (\mu^{11})^{-1} \mu^{12}), \\ b_{E_1}^3 &= K_1 (\chi^{13} - \chi^{11} (\mu^{11})^{-1} \mu^{13}), \end{aligned}$$

along with the following coefficients

$$\begin{aligned} K_1 &= (\varepsilon^{11} - \chi^{11} (\mu^{11})^{-1} \xi^{11})^{-1}, \\ K_2 &= (\mu^{11} - \xi^{11} (\varepsilon^{11})^{-1} \chi^{11})^{-1}, \\ K_3 &= -(\chi^{11} - \varepsilon^{11} (\xi^{11})^{-1} \mu^{11})^{-1}, \\ K_4 &= -(\xi^{11} - \mu^{11} (\chi^{11})^{-1} \varepsilon^{11})^{-1}. \end{aligned}$$

The coefficients  $K_i$  exhibit a common singularity (pole) governed by the condition

$$\varepsilon^{\tau\tau} \mu^{\tau\tau} - \chi^{\tau\tau} \xi^{\tau\tau} = 0, \quad (38)$$

where  $\tau = 1, 2$  indexes the component for which the Fourier expansion is performed. Consequently, the elements in the first and fourth rows of the matrix  $\tilde{Q}$ , specifically,  $\tilde{\varepsilon}^{1i}$ ,  $\tilde{\chi}^{1i}$ ,  $\tilde{\xi}^{1i}$ , and  $\tilde{\mu}^{1i}$ , are obtained via the Laurent's rule and the inverse rule and take the follow-

ing form:

$$\begin{cases} \tilde{\varepsilon}^{11} = \left[ \left( \varepsilon^{11} \right)^{-1} \right]^{-1}, \\ \tilde{\varepsilon}^{12} = \left[ \left( \varepsilon^{11} \right)^{-1} \right]^{-1} \left[ \left( \varepsilon^{11} \right)^{-1} \varepsilon^{12} \right], \\ \tilde{\varepsilon}^{13} = \left[ \left( \varepsilon^{11} \right)^{-1} \right]^{-1} \left[ \left( \varepsilon^{11} \right)^{-1} \varepsilon^{13} \right], \\ \tilde{\chi}^{11} = \left[ \left( \chi^{11} \right)^{-1} \right]^{-1}, \\ \tilde{\chi}^{12} = \left[ \left( \chi^{11} \right)^{-1} \right]^{-1} \left[ \left( \chi^{11} \right)^{-1} \chi^{12} \right], \\ \tilde{\chi}^{13} = \left[ \left( \chi^{11} \right)^{-1} \right]^{-1} \left[ \left( \chi^{11} \right)^{-1} \chi^{13} \right], \\ \tilde{\xi}^{11} = \left[ \left( \xi^{11} \right)^{-1} \right]^{-1}, \\ \tilde{\xi}^{12} = \left[ \left( \xi^{11} \right)^{-1} \right]^{-1} \left[ \left( \xi^{11} \right)^{-1} \xi^{12} \right], \\ \tilde{\xi}^{13} = \left[ \left( \xi^{11} \right)^{-1} \right]^{-1} \left[ \left( \xi^{11} \right)^{-1} \xi^{13} \right], \\ \tilde{\mu}^{11} = \left[ \left( \mu^{11} \right)^{-1} \right]^{-1}, \\ \tilde{\mu}^{12} = \left[ \left( \mu^{11} \right)^{-1} \right]^{-1} \left[ \left( \mu^{11} \right)^{-1} \mu^{12} \right], \\ \tilde{\mu}^{13} = \left[ \left( \mu^{11} \right)^{-1} \right]^{-1} \left[ \left( \mu^{11} \right)^{-1} \mu^{13} \right]. \end{cases}$$

In this notation, the brackets  $\llbracket \dots \rrbracket$  represent Toeplitz matrices constructed from the Fourier coefficients of the corresponding material parameters  $\varepsilon, \chi, \xi, \mu$ . The dimension of these matrices corresponds to the total number of harmonics used for the Fourier expansion along the  $x^1$ -axis. Next, to construct the second row of the matrix  $\tilde{Q}$ , the expressions for the field components  $E_1$  and  $H_1$  are substituted into the material equation for  $D^2$

$$\begin{aligned} D^2 &= \varepsilon^{2\sigma} E_\sigma + \chi^{2\sigma} H_\sigma = \\ &= \varepsilon^{21} E_1 + \varepsilon^{22} E_2 + \varepsilon^{23} E_3 + \chi^{21} H_1 + \chi^{22} H_2 + \chi^{23} H_3 = \\ &= \varepsilon^{21} \left[ e_{E_1}^1 D^1 - e_{E_1}^2 E_2 - e_{E_1}^3 E_3 - b_{E_1}^1 B^1 - b_{E_1}^2 H_2 - \right. \\ &\quad \left. - b_{E_1}^3 H_3 \right] + \varepsilon^{22} E_2 + \varepsilon^{23} E_3 + \\ &+ \chi^{21} \left[ -e_{H_1}^1 D^1 - e_{H_1}^2 E_2 - e_{H_1}^3 E_3 + b_{H_1}^1 B^1 - b_{H_1}^2 H_2 - \right. \\ &\quad \left. - b_{H_1}^3 H_3 \right] + \chi^{22} H_2 + \chi^{23} H_3 = \\ &= (\varepsilon^{21} e_{E_1}^1 - \chi^{21} e_{H_1}^1) D^1 + (\varepsilon^{22} - \varepsilon^{21} e_{E_1}^2 - \chi^{21} e_{H_1}^2) E_2 + \\ &\quad + (\varepsilon^{23} - \varepsilon^{21} e_{E_1}^3 - \chi^{21} e_{H_1}^3) E_3 + \\ &+ (-\varepsilon^{21} b_{E_1}^1 + \chi^{21} b_{H_1}^1) B^1 + (\chi^{22} - \varepsilon^{21} b_{E_1}^2 + \chi^{21} b_{H_1}^2) H_2 + \\ &\quad + (\chi^{23} - \varepsilon^{21} b_{E_1}^3 + \chi^{21} b_{H_1}^3) H_3. \end{aligned}$$

We now proceed to write the second row of the matrix

$\tilde{Q}$ . The components  $\tilde{\varepsilon}^{2\sigma}$  (for  $\sigma = 1, 2, 3$ ) originate from the constitutive relations connecting  $D^2$  and  $E_\sigma$ . Specifically, the component  $\tilde{\varepsilon}^{21}$  is derived from the relationship between  $D^2$  and  $E_1$ . This coupling appears in both the  $D^1$  and  $B^1$  components and should be written with the inverse rule

$$\begin{aligned} \varepsilon^{21} &= \llbracket \varepsilon^{21} e_{E_1}^1 - \chi^{21} e_{H_1}^1 \rrbracket \left[ \left( \varepsilon^{11} \right)^{-1} \right]^{-1} + \\ &+ \llbracket -\varepsilon^{21} b_{E_1}^1 + \chi^{21} b_{H_1}^1 \rrbracket \left[ \left( \xi^{11} \right)^{-1} \right]^{-1}. \end{aligned}$$

Next, the component  $\tilde{\varepsilon}^{22}$  is derived from the constitutive relation connecting  $D^2$  and  $E_2$ . This specific connection is represented in three distinct terms: within the material equation for  $D^1$  (36), within the material equation for  $B^1$  (36), and explicitly in the term preceding  $E_2$  in the original material equation. The expression for  $\tilde{\varepsilon}^{22}$  reads

$$\begin{aligned} \varepsilon^{22} &= \llbracket \varepsilon^{21} e_{E_1}^1 - \chi^{21} e_{H_1}^1 \rrbracket \left[ \left( \varepsilon^{11} \right)^{-1} \right]^{-1} \left[ \left( \varepsilon^{11} \right)^{-1} \varepsilon^{12} \right] + \\ &+ \llbracket -\varepsilon^{21} b_{E_1}^1 + \chi^{21} b_{H_1}^1 \rrbracket \left[ \left( \xi^{11} \right)^{-1} \right]^{-1} \left[ \left( \xi^{11} \right)^{-1} \xi^{12} \right]^{-1} + \\ &+ \llbracket \varepsilon^{22} - \varepsilon^{21} e_{E_1}^2 - \chi^{21} e_{H_1}^2 \rrbracket. \end{aligned}$$

Similarly, the component  $\tilde{\varepsilon}^{23}$  (from the  $D^2$ - $E_3$  relation) appears in three positions, namely, in the material equation for  $D^1$  (36), the material equation for  $B^1$  (36), and as the direct coefficient of  $E_3$ :

$$\begin{aligned} \varepsilon^{23} &= \llbracket \varepsilon^{21} e_{E_1}^1 - \chi^{21} e_{H_1}^1 \rrbracket \left[ \left( \varepsilon^{11} \right)^{-1} \right]^{-1} \left[ \left( \varepsilon^{11} \right)^{-1} \varepsilon^{13} \right] + \\ &+ \llbracket -\varepsilon^{21} b_{E_1}^1 + \chi^{21} b_{H_1}^1 \rrbracket \left[ \left( \xi^{11} \right)^{-1} \right]^{-1} \left[ \left( \xi^{11} \right)^{-1} \xi^{13} \right]^{-1} + \\ &+ \llbracket \varepsilon^{23} - \varepsilon^{21} e_{E_1}^3 - \chi^{21} e_{H_1}^3 \rrbracket. \end{aligned}$$

Next, the components  $\tilde{\chi}^{2\sigma}$  (for  $\sigma = 1, 2, 3$ ) originate from the constitutive relations between  $D^2$  and  $H_\sigma$ . Specifically, the component  $\tilde{\chi}^{21}$  is derived from the  $D^2$ - $H_1$  relation. This contribution is represented in two equations: those for  $D^1$  and  $B^1$ , yielding the following expression:

$$\begin{aligned} \chi^{21} &= \llbracket \varepsilon^{21} e_{E_1}^1 - \chi^{21} e_{H_1}^1 \rrbracket \left[ \left( \chi^{11} \right)^{-1} \right]^{-1} + \\ &+ \llbracket -\varepsilon^{21} b_{E_1}^1 + \chi^{21} b_{H_1}^1 \rrbracket \left[ \left( \mu^{11} \right)^{-1} \right]^{-1}. \end{aligned}$$

The component  $\tilde{\chi}^{22}$  is determined by the constitutive relation between  $D^2$  and  $H_2$ . This contribution manifests in three distinct terms: within the equation for  $D^1$ , within the equation for  $B^1$ , and explicitly as the coefficient preceding  $H_2$ :

$$\begin{aligned} \chi^{22} &= \llbracket \varepsilon^{21} e_{E_1}^1 - \chi^{21} e_{H_1}^1 \rrbracket \left[ \left( \chi^{11} \right)^{-1} \right]^{-1} \left[ \left( \chi^{11} \right)^{-1} \chi^{12} \right] + \\ &+ \llbracket -\varepsilon^{21} b_{E_1}^1 + \chi^{21} b_{H_1}^1 \rrbracket \left[ \left( \mu^{11} \right)^{-1} \right]^{-1} \left[ \left( \mu^{11} \right)^{-1} \mu^{12} \right]^{-1} + \\ &+ \llbracket \chi^{22} - \varepsilon^{21} b_{E_1}^2 - \chi^{21} b_{H_1}^2 \rrbracket. \end{aligned}$$

Finally,  $\tilde{\chi}^{23}$  (from the  $D^2$ - $H_3$  coupling) appears in three locations: in the  $D^1$  equation, the  $B^1$  equation, and as the direct coefficient of  $H_3$ .

$$\begin{aligned}\tilde{\chi}^{23} = & \llbracket \varepsilon^{21} e_{E_1}^1 - \chi^{21} e_{H_1}^1 \rrbracket \llbracket (\chi^{11})^{-1} \rrbracket^{-1} \llbracket (\chi^{11})^{-1} \chi^{13} \rrbracket + \\ & + \llbracket -\varepsilon^{21} b_{E_1}^1 + \chi^{21} b_{H_1}^1 \rrbracket \llbracket (\mu^{11})^{-1} \rrbracket^{-1} \llbracket (\mu^{11})^{-1} \mu^{13} \rrbracket^{-1} + \\ & + \llbracket \chi^{23} - \varepsilon^{21} b_{E_1}^3 - \chi^{21} b_{H_1}^3 \rrbracket.\end{aligned}$$

Having thus constructed the second row of the matrix  $\tilde{Q}$ , the remaining rows can be derived analogously by considering the corresponding material equations. The final explicit representation of the entire  $\tilde{Q}$  matrix is provided in Appendix XII

$$\tilde{Q} = \begin{pmatrix} \tilde{\varepsilon} & \tilde{\chi} \\ \tilde{\xi} & \tilde{\mu} \end{pmatrix} = \begin{pmatrix} \tilde{\varepsilon}^{11} & \tilde{\varepsilon}^{12} & \tilde{\varepsilon}^{13} & \tilde{\chi}^{11} & \tilde{\chi}^{12} & \tilde{\chi}^{13} \\ \tilde{\varepsilon}^{21} & \tilde{\varepsilon}^{22} & \tilde{\varepsilon}^{23} & \tilde{\chi}^{21} & \tilde{\chi}^{22} & \tilde{\chi}^{23} \\ \tilde{\varepsilon}^{31} & \tilde{\varepsilon}^{32} & \tilde{\varepsilon}^{33} & \tilde{\chi}^{31} & \tilde{\chi}^{32} & \tilde{\chi}^{33} \\ \tilde{\xi}^{11} & \tilde{\xi}^{12} & \tilde{\xi}^{13} & \tilde{\mu}^{11} & \tilde{\mu}^{12} & \tilde{\mu}^{13} \\ \tilde{\xi}^{21} & \tilde{\xi}^{22} & \tilde{\xi}^{23} & \tilde{\mu}^{21} & \tilde{\mu}^{22} & \tilde{\mu}^{23} \\ \tilde{\xi}^{31} & \tilde{\xi}^{32} & \tilde{\xi}^{33} & \tilde{\mu}^{31} & \tilde{\mu}^{32} & \tilde{\mu}^{33} \end{pmatrix}.$$

## XI. APPENDIX D. FOURIER TRANSFORM IN $x^2$

To handle two-dimensional periodicity, the formalism for the Fourier transform must be extended to the  $x^2$ -axis as well. The corresponding system of material equations for the case  $\rho = 2$  is the following

$$\begin{cases} D^2 = \varepsilon^{2\sigma} E_\sigma + \chi^{2\sigma} H_\sigma, \\ B^2 = \xi^{2\sigma} E_\sigma + \mu^{2\sigma} H_\sigma. \end{cases} \quad (39)$$

From the first equation of the system (39), we express the field component  $E_2$  and substitute it into the second equation. This allows us to determine the field component  $H_2$  via other field components  $E_1, D^2, E_3, H_1, B^2, H_3$ :

$$\begin{aligned}H_2 = & (\mu^{22} - \xi^{22}(\varepsilon^{22})^{-1}\chi^{22})^{-1} \left[ -(\xi^{21} - \xi^{22}(\varepsilon^{22})^{-1}\varepsilon^{21}) E_1 - \right. \\ & - \xi^{22}(\varepsilon^{22})^{-1} D^2 - (\xi^{23} - \xi^{22}(\varepsilon^{22})^{-1}\varepsilon^{23}) E_3 + \\ & - (\mu^{21} - \xi^{22}(\varepsilon^{22})^{-1}\chi^{21}) H_1 + B^2 - \\ & \left. - (\mu^{23} - \xi^{22}(\varepsilon^{22})^{-1}\chi^{23}) H_3 \right].\end{aligned}$$

Solving the second equation for  $H_2$  and substituting into the first equation provides us an expression for the  $E_2$  in

terms of  $E_1, D^2, E_3, H_1, B^2, H_3$ :

$$\begin{aligned}E_2 = & (\varepsilon^{22} - \chi^{22}(\mu^{22})^{-1}\xi^{22})^{-1} \left[ -(\varepsilon^{21} - \chi^{22}(\mu^{22})^{-1}\xi^{21}) E_1 + \right. \\ & + D^2 - (\varepsilon^{23} - \chi^{22}(\mu^{22})^{-1}\xi^{23}) E_3 - \\ & - (\chi^{21} - \chi^{22}(\mu^{22})^{-1}\mu^{21}) H_1 - \chi^{22}(\mu^{22})^{-1} B^2 - \\ & \left. - (\chi^{23} - \chi^{22}(\mu^{22})^{-1}\mu^{23}) H_3 \right].\end{aligned}$$

Briefly, we can write that

$$\begin{aligned}H_2 = & -\tilde{e}_{H_2}^1 E_1 - \tilde{e}_{H_2}^2 D^2 - \tilde{e}_{H_2}^3 E_3 - \tilde{b}_{H_2}^1 H_1 + \tilde{b}_{H_2}^2 B^2 - \tilde{b}_{H_2}^3 H_3, \\ E_2 = & -\tilde{e}_{E_2}^1 E_1 + \tilde{e}_{E_2}^2 D^2 - \tilde{e}_{E_2}^3 E_3 - \tilde{b}_{E_2}^1 H_1 - \tilde{b}_{E_2}^2 B^2 - \tilde{b}_{E_2}^3 H_3.\end{aligned}$$

where new symbols are introduced

$$\begin{aligned}\tilde{e}_{H_1}^1 &= \widetilde{K}_2 (\xi^{21} - \xi^{22}(\varepsilon^{22})^{-1}\varepsilon^{21}), \\ \tilde{e}_{H_1}^2 &= \widetilde{K}_2 \xi^{22}(\varepsilon^{22})^{-1} = -\widetilde{K}_3, \\ \tilde{e}_{H_1}^3 &= \widetilde{K}_2 (\xi^{23} - \xi^{22}(\varepsilon^{22})^{-1}\varepsilon^{23}), \\ \tilde{b}_{H_1}^1 &= \widetilde{K}_2 (\mu^{21} - \xi^{22}(\varepsilon^{22})^{-1}\chi^{21}), \\ \tilde{b}_{H_1}^2 &= \widetilde{K}_2, \\ \tilde{b}_{H_1}^3 &= \widetilde{K}_2 (\mu^{23} - \xi^{22}(\varepsilon^{22})^{-1}\chi^{23}), \\ \tilde{e}_{E_1}^1 &= \widetilde{K}_1 (\varepsilon^{21} - \chi^{22}(\mu^{22})^{-1}\xi^{21}), \\ \tilde{e}_{E_1}^2 &= \widetilde{K}_1, \\ \tilde{e}_{E_1}^3 &= \widetilde{K}_1 (\varepsilon^{23} - \chi^{22}(\mu^{22})^{-1}\xi^{23}), \\ \tilde{b}_{E_1}^1 &= \widetilde{K}_1 (\chi^{21} - \chi^{22}(\mu^{22})^{-1}\mu^{21}), \\ \tilde{b}_{E_1}^2 &= \widetilde{K}_1 \chi^{22}(\mu^{22})^{-1} = -\widetilde{K}_4, \\ \tilde{b}_{E_1}^3 &= \widetilde{K}_1 (\chi^{23} - \chi^{22}(\mu^{22})^{-1}\mu^{23}),\end{aligned}$$

along with the following coefficients

$$\begin{aligned}\widetilde{K}_1 &= (\varepsilon^{22} - \chi^{22}(\mu^{22})^{-1}\xi^{22})^{-1}, \\ \widetilde{K}_2 &= (\mu^{22} - \xi^{22}(\varepsilon^{22})^{-1}\chi^{22})^{-1}, \\ \widetilde{K}_3 &= -(\chi^{22} - \varepsilon^{22}(\xi^{22})^{-1}\mu^{22})^{-1}, \\ \widetilde{K}_4 &= -(\xi^{22} - \mu^{22}(\chi^{22})^{-1}\varepsilon^{22})^{-1}.\end{aligned}$$

Here, the same pole condition as in (38) appears, but now for the component  $\tau = 2$ . The second and fourth rows of the matrix  $\tilde{Q}$ , namely, the elements  $\tilde{\varepsilon}^{2i}, \tilde{\chi}^{2i}, \tilde{\xi}^{2i}$ , and  $\tilde{\mu}^{2i}$ , are constructed directly by applying Laurent's

rule and the inverse rule

$$\begin{cases} \hat{\varepsilon}^{21} = \left[ \left( \tilde{\varepsilon}^{22} \right)^{-1} \right]^{-1} \left[ \left( \tilde{\varepsilon}^{22} \right)^{-1} \tilde{\varepsilon}^{21} \right], \\ \hat{\varepsilon}^{22} = \left[ \left( \tilde{\varepsilon}^{22} \right)^{-1} \right]^{-1}, \\ \hat{\varepsilon}^{23} = \left[ \left( \tilde{\varepsilon}^{22} \right)^{-1} \right]^{-1} \left[ \left( \tilde{\varepsilon}^{22} \right)^{-1} \tilde{\varepsilon}^{23} \right], \\ \hat{\chi}^{21} = \left[ \left( \tilde{\chi}^{22} \right)^{-1} \right]^{-1} \left[ \left( \tilde{\chi}^{22} \right)^{-1} \tilde{\chi}^{21} \right], \\ \hat{\chi}^{22} = \left[ \left( \tilde{\chi}^{22} \right)^{-1} \right]^{-1}, \\ \hat{\chi}^{23} = \left[ \left( \tilde{\chi}^{22} \right)^{-1} \right]^{-1} \left[ \left( \tilde{\chi}^{22} \right)^{-1} \tilde{\chi}^{23} \right], \\ \hat{\xi}^{21} = \left[ \left( \tilde{\xi}^{22} \right)^{-1} \right]^{-1} \left[ \left( \tilde{\xi}^{22} \right)^{-1} \tilde{\xi}^{21} \right], \\ \hat{\xi}^{22} = \left[ \left( \tilde{\xi}^{22} \right)^{-1} \right]^{-1}, \\ \hat{\xi}^{23} = \left[ \left( \tilde{\xi}^{22} \right)^{-1} \right]^{-1} \left[ \left( \tilde{\xi}^{22} \right)^{-1} \tilde{\xi}^{23} \right], \\ \hat{\mu}^{21} = \left[ \left( \tilde{\mu}^{22} \right)^{-1} \right]^{-1} \left[ \left( \tilde{\mu}^{22} \right)^{-1} \tilde{\mu}^{21} \right], \\ \hat{\mu}^{22} = \left[ \left( \tilde{\mu}^{22} \right)^{-1} \right]^{-1}, \\ \hat{\mu}^{23} = \left[ \left( \tilde{\mu}^{22} \right)^{-1} \right]^{-1} \left[ \left( \tilde{\mu}^{22} \right)^{-1} \tilde{\mu}^{23} \right], \end{cases}$$

Dimensionality of these matrices is  $N_g \times N_g$ . The elements of the matrix  $\hat{Q}$  are constructed analogously to the case of the  $x^1$ -axis, following the methodology outlined previously. The final form of the matrix is given in Appendix XII

$$\hat{Q} = \begin{pmatrix} \hat{\varepsilon} & \hat{\chi} \\ \hat{\xi} & \hat{\mu} \end{pmatrix} = \begin{pmatrix} \hat{\varepsilon}^{11} & \hat{\varepsilon}^{12} & \hat{\varepsilon}^{13} & \hat{\chi}^{11} & \hat{\chi}^{12} & \hat{\chi}^{13} \\ \hat{\varepsilon}^{21} & \hat{\varepsilon}^{22} & \hat{\varepsilon}^{23} & \hat{\chi}^{21} & \hat{\chi}^{22} & \hat{\chi}^{23} \\ \hat{\varepsilon}^{31} & \hat{\varepsilon}^{32} & \hat{\varepsilon}^{33} & \hat{\chi}^{31} & \hat{\chi}^{32} & \hat{\chi}^{33} \\ \hat{\xi}^{11} & \hat{\xi}^{12} & \hat{\xi}^{13} & \hat{\mu}^{11} & \hat{\mu}^{12} & \hat{\mu}^{13} \\ \hat{\xi}^{21} & \hat{\xi}^{22} & \hat{\xi}^{23} & \hat{\mu}^{21} & \hat{\mu}^{22} & \hat{\mu}^{23} \\ \hat{\xi}^{31} & \hat{\xi}^{32} & \hat{\xi}^{33} & \hat{\mu}^{31} & \hat{\mu}^{32} & \hat{\mu}^{33} \end{pmatrix}.$$

## XII. APPENDIX E. EXPLICIT FORM OF $\tilde{Q}$ AND $\hat{Q}$ MATRICES

The explicit form of the elements of the  $6 \times 6$  block matrices  $\tilde{Q}$  and  $\hat{Q}$

$$\tilde{Q} = \begin{pmatrix} \tilde{\varepsilon} & \tilde{\chi} \\ \tilde{\xi} & \tilde{\mu} \end{pmatrix}, \quad \hat{Q} = \begin{pmatrix} \hat{\varepsilon} & \hat{\chi} \\ \hat{\xi} & \hat{\mu} \end{pmatrix} \quad (40)$$

is the following:

$$\begin{cases} \tilde{\varepsilon}^{11} = \left[ \left( \varepsilon^{11} \right)^{-1} \right]^{-1}, \\ \tilde{\varepsilon}^{12} = \left[ \left( \varepsilon^{11} \right)^{-1} \right]^{-1} \left[ \left( \varepsilon^{11} \right)^{-1} \varepsilon^{12} \right], \\ \tilde{\varepsilon}^{13} = \left[ \left( \varepsilon^{11} \right)^{-1} \right]^{-1} \left[ \left( \varepsilon^{11} \right)^{-1} \varepsilon^{13} \right], \\ \tilde{\varepsilon}^{21} = \left[ \varepsilon^{21} e_{E_1}^1 - \chi^{21} e_{H_1}^1 \right] \left[ \left( \varepsilon^{11} \right)^{-1} \right]^{-1} + \\ + \left[ -\varepsilon^{21} b_{E_1}^1 + \chi^{21} b_{H_1}^1 \right] \left[ \left( \varepsilon^{11} \right)^{-1} \right]^{-1}, \\ \tilde{\varepsilon}^{22} = \left[ \varepsilon^{21} e_{E_1}^1 - \chi^{21} e_{H_1}^1 \right] \left[ \left( \varepsilon^{11} \right)^{-1} \right]^{-1} \left[ \left( \varepsilon^{11} \right)^{-1} \varepsilon^{12} \right] + \\ + \left[ -\varepsilon^{21} b_{E_1}^1 + \chi^{21} b_{H_1}^1 \right] \left[ \left( \varepsilon^{11} \right)^{-1} \right]^{-1} \left[ \left( \varepsilon^{11} \right)^{-1} \varepsilon^{12} \right] + \\ + \left[ \varepsilon^{22} - \varepsilon^{21} e_{E_1}^2 - \chi^{21} e_{H_1}^2 \right], \\ \tilde{\varepsilon}^{23} = \left[ \varepsilon^{21} e_{E_1}^1 - \chi^{21} e_{H_1}^1 \right] \left[ \left( \varepsilon^{11} \right)^{-1} \right]^{-1} \left[ \left( \varepsilon^{11} \right)^{-1} \varepsilon^{13} \right] + \\ + \left[ -\varepsilon^{21} b_{E_1}^1 + \chi^{21} b_{H_1}^1 \right] \left[ \left( \varepsilon^{11} \right)^{-1} \right]^{-1} \left[ \left( \varepsilon^{11} \right)^{-1} \varepsilon^{13} \right] + \\ + \left[ \varepsilon^{23} - \varepsilon^{21} e_{E_1}^3 - \chi^{21} e_{H_1}^3 \right], \\ \tilde{\varepsilon}^{31} = \left[ \varepsilon^{31} e_{E_1}^1 - \chi^{31} e_{H_1}^1 \right] \left[ \left( \varepsilon^{11} \right)^{-1} \right]^{-1} + \\ + \left[ -\varepsilon^{31} b_{E_1}^1 + \chi^{31} b_{H_1}^1 \right] \left[ \left( \varepsilon^{11} \right)^{-1} \right]^{-1}, \\ \tilde{\varepsilon}^{32} = \left[ \varepsilon^{31} e_{E_1}^1 - \chi^{31} e_{H_1}^1 \right] \left[ \left( \varepsilon^{11} \right)^{-1} \right]^{-1} \left[ \left( \varepsilon^{11} \right)^{-1} \varepsilon^{12} \right] + \\ + \left[ -\varepsilon^{31} b_{E_1}^1 + \chi^{31} b_{H_1}^1 \right] \left[ \left( \varepsilon^{11} \right)^{-1} \right]^{-1} \left[ \left( \varepsilon^{11} \right)^{-1} \varepsilon^{12} \right] + \\ + \left[ \varepsilon^{32} - \varepsilon^{31} e_{E_1}^2 - \chi^{31} e_{H_1}^2 \right], \\ \tilde{\varepsilon}^{33} = \left[ \varepsilon^{31} e_{E_1}^1 - \chi^{31} e_{H_1}^1 \right] \left[ \left( \varepsilon^{11} \right)^{-1} \right]^{-1} \left[ \left( \varepsilon^{11} \right)^{-1} \varepsilon^{13} \right] + \\ + \left[ -\varepsilon^{31} b_{E_1}^1 + \chi^{31} b_{H_1}^1 \right] \left[ \left( \varepsilon^{11} \right)^{-1} \right]^{-1} \left[ \left( \varepsilon^{11} \right)^{-1} \varepsilon^{13} \right] + \\ + \left[ \varepsilon^{33} - \varepsilon^{31} e_{E_1}^3 - \chi^{31} e_{H_1}^3 \right], \\ \tilde{\chi}^{11} = \left[ \left( \chi^{11} \right)^{-1} \right]^{-1}, \\ \tilde{\chi}^{12} = \left[ \left( \chi^{11} \right)^{-1} \right]^{-1} \left[ \left( \chi^{11} \right)^{-1} \chi^{12} \right], \\ \tilde{\chi}^{13} = \left[ \left( \chi^{11} \right)^{-1} \right]^{-1} \left[ \left( \chi^{11} \right)^{-1} \chi^{13} \right], \\ \tilde{\chi}^{21} = \left[ \varepsilon^{21} e_{E_1}^1 - \chi^{21} e_{H_1}^1 \right] \left[ \left( \chi^{11} \right)^{-1} \right]^{-1} + \\ + \left[ -\varepsilon^{21} b_{E_1}^1 + \chi^{21} b_{H_1}^1 \right] \left[ \left( \mu^{11} \right)^{-1} \right]^{-1}, \\ \tilde{\chi}^{22} = \left[ \varepsilon^{21} e_{E_1}^1 - \chi^{21} e_{H_1}^1 \right] \left[ \left( \chi^{11} \right)^{-1} \right]^{-1} \left[ \left( \chi^{11} \right)^{-1} \chi^{12} \right] + \\ + \left[ -\varepsilon^{21} b_{E_1}^1 + \chi^{21} b_{H_1}^1 \right] \left[ \left( \mu^{11} \right)^{-1} \right]^{-1} \left[ \left( \mu^{11} \right)^{-1} \mu^{12} \right] + \\ + \left[ -\varepsilon^{21} b_{E_1}^2 - \chi^{21} b_{H_1}^2 + \chi^{22} \right], \\ \tilde{\chi}^{23} = \left[ \varepsilon^{21} e_{E_1}^1 - \chi^{21} e_{H_1}^1 \right] \left[ \left( \chi^{11} \right)^{-1} \right]^{-1} \left[ \left( \chi^{11} \right)^{-1} \chi^{13} \right] + \\ + \left[ -\varepsilon^{21} b_{E_1}^1 + \chi^{21} b_{H_1}^1 \right] \left[ \left( \mu^{11} \right)^{-1} \right]^{-1} \left[ \left( \mu^{11} \right)^{-1} \mu^{13} \right] + \\ + \left[ -\varepsilon^{21} b_{E_1}^3 - \chi^{21} b_{H_1}^3 + \chi^{23} \right], \\ \tilde{\chi}^{31} = \left[ \varepsilon^{31} e_{E_1}^1 - \chi^{31} e_{H_1}^1 \right] \left[ \left( \chi^{11} \right)^{-1} \right]^{-1} + \\ + \left[ -\varepsilon^{31} b_{E_1}^1 + \chi^{31} b_{H_1}^1 \right] \left[ \left( \mu^{11} \right)^{-1} \right]^{-1}, \\ \tilde{\chi}^{32} = \left[ \varepsilon^{31} e_{E_1}^1 - \chi^{31} e_{H_1}^1 \right] \left[ \left( \chi^{11} \right)^{-1} \right]^{-1} \left[ \left( \chi^{11} \right)^{-1} \chi^{12} \right] + \\ + \left[ -\varepsilon^{31} b_{E_1}^1 + \chi^{31} b_{H_1}^1 \right] \left[ \left( \mu^{11} \right)^{-1} \right]^{-1} \left[ \left( \mu^{11} \right)^{-1} \mu^{12} \right] + \\ + \left[ -\varepsilon^{31} b_{E_1}^2 - \chi^{31} b_{H_1}^2 + \chi^{32} \right], \\ \tilde{\chi}^{33} = \left[ \varepsilon^{31} e_{E_1}^1 - \chi^{31} e_{H_1}^1 \right] \left[ \left( \chi^{11} \right)^{-1} \right]^{-1} \left[ \left( \chi^{11} \right)^{-1} \chi^{13} \right] + \\ + \left[ -\varepsilon^{31} b_{E_1}^1 + \chi^{31} b_{H_1}^1 \right] \left[ \left( \mu^{11} \right)^{-1} \right]^{-1} \left[ \left( \mu^{11} \right)^{-1} \mu^{13} \right] + \\ + \left[ -\varepsilon^{31} b_{E_1}^3 - \chi^{31} b_{H_1}^3 + \chi^{33} \right], \end{cases}$$







- 
- [1] M. Moharam and T. Gaylord, Rigorous coupled-wave analysis of planar-grating diffraction., *JOSA*, **71**(7), 811-818. (1981).
- [2] S. Tikhodeev, A. Y. E.A., M. N. Gippius, and T. Ishihara, Quasiguided modes and optical properties of photonic crystal slabs., *Physical Review B*, **66**(4), 045102. (2002).
- [3] I. M. Fradkin, S. A. Dyakov, and N. A. Gippius, Nanoparticle lattices with bases: Fourier modal method and dipole approximation, *Physical Review B* **102**, 045432 (2020).
- [4] N. S. Salakhova, I. M. Fradkin, S. A. Dyakov, and N. A. Gippius, Fourier modal method for moiré lattices, *Physical Review B* **104**, 085424 (2021).
- [5] W. C. Johnson, Secondary structure of proteins through circular dichroism spectroscopy, *Annual Review of Biophysics and Biophysical Chemistry* **17**, 145 (1988).
- [6] E. Hendry, T. Carpy, J. Johnston, M. Popland, R. V. Mikhaylovskiy, A. J. Lapthorn, S. M. Kelly, L. D. Barron, N. Gadegaard, and M. Kadodwala, Ultrasensitive detection and characterization of biomolecules using superchiral fields, *Nature Nanotechnology* **5**, 783 (2010).
- [7] Y. Tang and A. E. Cohen, Enhanced enantioselectivity in excitation of chiral molecules by superchiral light, *Science* **332**, 333 (2011).
- [8] Y. Inoue and V. Ramamurthy, *Chiral photochemistry* (CRC Press, 2004).
- [9] I. Hodgkinson and Q. h. Wu, Inorganic chiral optical materials, *Advanced materials* **13**, 889 (2001).
- [10] F. Fyodorov, *Teoriya girotropii* (1976).
- [11] I. Lindell, A. Sihvola, S. Tretyakov, and A. J. Viitanen, *Electromagnetic waves in chiral and bi-isotropic media* (Artech House, 1994).
- [12] S. Almousa, T. Weiss, and E. Muljarov, Employing quasidegenerate optical modes for chiral sensing, *Physical Review B* **109**, L041410 (2024).
- [13] F. Nutsch, E. Barredo-Alamilla, and M. A. Gorchach, Complex-valued tellegen response, *Applied Physics Letters* **126** (2025).
- [14] S. A. Dyakov, N. S. Salakhova, A. V. Ignatov, I. M. Fradkin, V. P. Panov, J.-K. Song, and N. A. Gippius, Chiral light in twisted fabry-pérot cavities, *Advanced Optical Materials* **12**, 2302502 (2024).
- [15] L. Li, Use of fourier series in the analysis of discontinuous periodic structures, *Journal of the Optical Society of America A*, **13**(9), 1870. (1996).
- [16] L. . Li, Reformulation of the fourier modal method for surface-relief gratings made with anisotropic materials, *Journal of Modern Optics*, **45**(7), 1313-1334. (1998).
- [17] L. Li, Fourier modal method for crossed anisotropic gratings with arbitrary permittivity and permeability tensors, *Journal of Optics A: Pure and Applied Optics*, **5**(4), 345-355. (2003).
- [18] R. Redheffer, Inequalities for a matrix riccati equation, *Journal of Mathematics and Mechanics* , 349 (1959).
- [19] R. C. Rumpf, Improved formulation of scattering matrices for semi-analytical methods that is consistent with convention, *Progress In Electromagnetics Research B* **35**, 241 (2011).
- [20] B. E. Saleh and M. C. Teich, *Fundamentals of photonics, 2 volume set* (John Wiley & sons, 2019).
- [21] C. Simovski, *Composite Media with Weak Spatial Dispersion* (Jenny Stanford Publishing, 2018).
- [22] G.-G. Liu, S. Mandal, X. Xi, Q. Wang, C. Devescovi, A. Morales-Pérez, Z. Wang, L. Yang, R. Banerjee, Y. Long, *et al.*, Photonic axion insulator, *Science* **387**, 162 (2025).
- [23] Q. Yang, X. Wen, Z. Li, O. You, and S. Zhang, Gigantic tellegen responses in metamaterials, *Nature Communications* **16**, 151 (2025).
- [24] S. Safaei Jazi, I. Faniaye, R. Cicheler, D. C. Tzarouchis, M. M. Asgari, A. Dmitriev, S. Fan, and V. Asadchy, Optical tellegen metamaterial with spontaneous magnetization, *Nature Communications* **15**, 1293 (2024).
- [25] L. Shaposhnikov, M. Mazanov, D. A. Bobylev, F. Wilczek, and M. A. Gorchach, Emergent axion response in multilayered metamaterials, *Physical Review B* **108**, 115101 (2023).
- [26] T. Z. Seidov and M. A. Gorchach, Unbounded tellegen response in media with multiple resonances, *Physical Review A* **111**, 033521 (2025).
- [27] W. Brown Jr, R. Hornreich, and S. Shtrikman, Upper bound on the magnetoelectric susceptibility, *Physical Review* **168**, 574 (1968).
- [28] J. Lekner, Optical properties of isotropic chiral media, *Pure and Applied Optics: Journal of the European Optical Society Part A* **5**, 417 (1996).
- [29] Y. Tang and A. E. Cohen, Optical chirality and its interaction with matter, *Physical Review Letters* **104**, 163901 (2010).
- [30] S. Dyakov, I. Smagin, N. Salakhova, O. Blokhin, D. G. Baranov, I. Fradkin, and N. Gippius, Strong coupling of chiral light with chiral matter: a macroscopic study, *Optica* **12**, 1406 (2025).
- [31] S. Dyakov, N. Gippius, I. Fradkin, and S. Tikhodeev, Vertical routing of spinning-dipole radiation from a chiral metasurface, *Physical Review Applied* **14**, 024090 (2020).
- [32] I. M. Fradkin, A. A. Demenev, A. V. Kovalchuk, V. D. Kulakovskii, V. N. Antonov, S. A. Dyakov, and N. A. Gippius, Nearly perfect routing of chiral light by plasmonic grating on slab waveguide, *arXiv preprint arXiv:2312.05865* (2023).
- [33] J. Petersen, J. Volz, and A. Rauschenbeutel, Chiral nanophotonic waveguide interface based on spin-orbit interaction of light, *Science* **346**, 67 (2014).
- [34] D. G. Baranov, C. Schäfer, and M. V. Gorkunov, Toward molecular chiral polaritons, *ACS Photonics* **10**, 2440 (2023).
- [35] W. Chen, Z. Wang, and M. Gorkunov, Uncovering maximum chirality in resonant nanostructures, *Nano Lett.*, **24**, 9643-9649 (2024).